NACA TM 1220

7881

TECH LIBRARY KAFB, NM
0144541

NATIONAL ADVISORY COMMITTEE FOR AERONAUTICS

TECHNICAL MEMORANDUM 1220

PRESSURE-DISTRIBUTION MEASUREMENTS ON THE TAIL SURFACES OF A ROTATING MODEL OF THE DESIGN BFW - M 31

By M. Kohler and W. Mautz

Translation of ZWB Forschungsbericht Nr. 704, Göttingen, September 30, 1936.

Washington
December 1949

ARMDC
TECHNICAL LIBRARY
AFL 2811

ZM 98/12

TECH LIBRARY KAFB, NM
0144541

NATIONAL ADVISORY COMMITTEE FOR AERONAUTICS

TECHNICAL MEMORANDUM 1220

PRESSURE-DISTRIBUTION MEASUREMENTS ON THE TAIL SURFACES OF A ROTATING MODEL OF THE DESIGN BFW - M 31*

By M. Kohler and W. Mautz

ABSTRACT: In order to obtain insight into the flow conditions on tail surfaces of airplanes during spins, pressure-distribution measurements were performed on a rotating model of the design BFW - M 31. For the time being, the tests were made for only one angle of attack ($\alpha = 60°$) and various angles of yaw and rudder angles. The results of these measurements are given; the construction of the model, and the test arrangement used are described. Measurements to be performed later and alterations planned in the test arrangement are pointed out.

OUTLINE:

I. INTRODUCTION

II. PRINCIPLES THE TESTS ARE BASED ON

III. DESCRIPTION OF THE TEST ARRANGEMENT
1. Construction of the Model
2. Driving Unit
3. Pressure Transfer

IV. REPRESENTATION OF THE TEST RESULTS
1. Evaluation, Corrections
2. Plotting of the Measured Pressures, Definitions

V. DISCUSSION OF THE RESULTS

VI. INDICATION OF FURTHER MEASUREMENTS TO BE PERFORMED WITH A TEST ARRANGEMENT ALREADY BEING DEVELOPED

VII. SUMMARY

---

*"Druckverteilungsmessungen am Leitwerk eines rotierenden Modelles des Flugzeugmusters BFW - M 31." Zentrale für wissenschaftliches Berichtswesen über Luftfahrtforschung, Forschungsbericht Nr. 704, Göttingen, September 30, 1936.

I. INTRODUCTION

Knowledge of the flow phenomena at the tail surfaces for stalled flight condition, particularly for an added rotary motion, is of fundamental importance for the study of the problem of spin. Above all, the shielding effect of fuselage and horizontal tail surfaces on the vertical tail surfaces is of interest. Force measurements yield only integral values and show little concerning the nature of the flow phenomena. For a better understanding of the flow conditions at the tail surfaces one must depend on the experimental determination of the pressure distribution. The following report brings the results of such a measurement. It is, so far, only a matter of preliminary tests which are to serve as a basis for later tests and, on the basis of gained experience, to indicate how future measurements of a similar kind should be performed.

II. PRINCIPLES THE TESTS ARE BASED ON

For these measurements an airplane design was selected which showed inclination for flat spins and on which at the same time flying tests were performed elsewhere. The design in question is the BFW - M 31.

The first tests were performed with standard tail surfaces. However, later investigations of various types of tail surfaces on the same model are intended.

III. DESCRIPTION OF THE TEST ARRANGEMENT

1. Construction of the Model

The model of the airplane design investigated was built in an all-metal construction on the scale 1:10 according to data of the firm Bayerische Flugzeugwerke A.-G. Augsburg. Two reasons were decisive for metal construction:

a. great mechanical strain by mass forces

b. desire for freedom from deformation since the measurements will extend over a long period of time

Figure 1 represents a survey diagram of the model showing the main dimensions. The two wing halves were roughed by hammering two pieces of 3 mm thick aluminum foil, and welded at the nose and trailing edge. The final forming was done by hand according to templet. The fuselage was manufacted of silicon-aluminum alloy casting and was also hand-finished.

In order to confine the flow disturbance, for all conditions investigated, to the narrowest possible limits one aimed at placing the parts of the attachment of the model on the drive shaft and those serving for adjustment of the angles of attack and of yaw into the fuselage of the model. Figure 2 shows a sectional drawing of the model, showing the construction details. The connection with the drive shaft was made as follows: a fork end of high-grade steel is bolted to a base plate which transfers the forces directly onto the model. The fork has a boring and a slot for a wedged pin connecting the fork with the shaft-connection piece and an adapter. This connection simultaneously offers the possibility of adjusting the angle of attack. The shaft connection piece has an internal gearing into which the adapter interlocks with a corresponding counter gearing. Every shifting by one tooth corresponds to an angle variation of 10°. For the possibility of adjustment of intermediary values the adapter was furnished with a second slot for the connecting wedge which is displaced by 85° relative to the first. By suitable installation of the adapter and insertion of the wedge into the second slot the values 35°, 45°, etc. may then be adjusted so that the model can be connected to the drive shaft from 30° to 90° in intervals of 5°. For an arrangement with the drive shaft passing through the center of gravity, smaller values than 30° cannot be attained with a straight shaft since the vertical tail surfaces would interfere with the drive shaft. The use of a cam shaft made a lighter model construction necessary which was given up for the time being, due to the reasons given in III, 1 a and b.

The angle of yaw is arbitrarily adjustable within the limits -10° to + 10°. The adjusting device is, briefly, as follows: The base plate of the fork end carries two oblique slots (see fig. 2). Two pins interlock in these slots the rectangular base of which is fitted into a groove of the base plate. The base is bored through and furnished with right-hand and left-hand thread, respectively. By means of a spindle which also shows right-hand and left-hand thread and is placed at the base plate the pins may be moved in the slots toward the outside or inside. Thereby the fork itself is rotated about its vertical axis and the angle of yaw is altered. The torque to be absorbed is transferred by the pins to the fork in every position without changes. The shaft joint coupling is fixed to the drive shaft by a coupling nut; the torque is at this point transferred by a wedge.

Figure 3 shows a photograph of the model with the upper fuselage shell taken off. In order to show the attachment of the wings to the fuselage, the cover plate has been removed from the upper side of the left wing. The partial section represented in figure 4 shows above all the fork end and the spindle for adjustment of the angle of yaw.

The fuselage end with the tail-surface areas was built in an interchangeable construction. The framework of the tail fins was attached to this hollow tail piece (see fig. 5). The frame work of such a fin consists of a brass frame rigidly connected with ribs of the same material and with

brass tubules of 2 mm thickness. The measuring bore holes lie, in each case, in a rib and enter into the tubules which transmit the pressures. The interspaces of the tail-surface framework were filled up with a synthetic marble mass and after hardening finished as a whole with the ribs.

The control surfaces were manufactured in the same manner and pivoted to the fins with a continuous bolt. After removal of the adapters visible in the photograph the bolt may be inserted at the control-surface ends. By tightening the bolt, the control surfaces may be locked in any desired position (control-surface deflections are possible up to $\pm 25^{\circ}$). The pressure lines were developed flexible by attachment of a valve-tubing connection at the center of rotation of the control-surface axis; they were led through the hollow end of the fuselage to a control panel in the interior of the divided fuselage. Hence the connection with the lines in the interior of the drive shaft which protruded from a slot at the shaft end was made, also by valve tubing.

Since only a limited number of lines could be placed in the interior of the hollow fuselage end, only one side of the vertical tail surfaces was provided with measuring bore holes. The bore holes on the horizontal tail surfaces were made on one half on the upper side, on the other on the lower side. The pressures on the sides without bore holes were determined by reversing the direction of rotation as well as angle of yaw and rudder angle of the model (in case the latter were different from 0°) and performing the measurement again on the side first measured.

The photograph, figure 6, shows the complete model with the shaft connection piece.

2. Driving Unit

The model was driven by means of a test device developed previously for pressure distribution measurements on rotating wings. It consists essentially of two parts: a rigid bearing pedestal and a drive shaft held by wire braces and resting in two ball bearings fastened in a tube. An elastic coupling connects the two parts.

In the rear part of the rigid bearing pedestal are Fuhrmann gaskets (see following paragraph); with their aid the pressures were transmitted from the rotating system. In the front part of this bearing pedestal there are placed, above and below, the sprocket wheels serving for transfer of the torque of the motor onto the drive shaft. The driving unit with a rpm-counter is in the test section below the free jet.

An adjustable counterweight is fastened to the drive shaft between the rear bearings and the elastic coupling which serves for the static

compensation of the weights of the rotating system. Moreover, a worm with worm wheel is situated there which serves as revolution indicator.

Figure 7[1] shows the installation of the model in the test section of the wind tunnel K IV (1500 mm nozzle diameter) of the Aerodynamischen Versuchsanstalt. The photograph shows the bearing block with the gaskets and the drive shaft braced in front of it. In the lower part of the figure one sees the chain leading to the driving unit. The tubing connected with the manometer also is clearly visible.

3. Pressure Transfer

In order to transfer the pressures from the rotating system to the stationary manometer, gaskets of the Fuhrmann type were used (see Fuhrmann: "Untersuchungen an einem Propellermodell" [Investigations on a Propeller Model]. ZFM 1913, Nr. 4, p. 89, and also Flachsbart: "Luftschrauben" [Propellers]. Handb. d. Exp. Phys., Bd. 4, 3. Teil, p. 385). These gaskets, in a slightly altered form, stood up well in the tests, except that their total length did not permit the use of an arbitrary number in series.

Since for the present case only 9 gaskets were at disposal and any greater number is difficult to install, application of a multiple manometer was omitted and the pressures were conveyed individually each to a Prandtl manometer. The somewhat greater time expenditure in this case was compensated by the simplified evaluation. Every group of 9 pressures which could be measured simultaneously pertained to a tail-surface section. The boreholes of the other sections - which opened into the same ducts - were sealed with a plastic mass (Stauffer grease and beeswax). It should be mentioned that the sources of error increase with the number of gaskets so that it seems advisable to reduce the measuring time by another method (see section VI).

A detailed description of the driving unit and the gaskets will be published in a later report by M. Kohler: "Druckverteilungen an rotierenden Tragflügeln" (Pressure distributions on rotating wings.)

IV. REPRESENTATION OF THE TEST RESULTS

1. Evaluation, Corrections

The pressures measured on the rotating model required a correction since the air mass in the interior of the ducting is subjected to centrifugal forces. Due to the effect of the centrifugal forces the reading of the

[1]This figure was totally indistinguishable in the only available copy of the original German document; therefore, it was not reproduced in the translated version.

positive pressures was too low, that of the negative pressures too high, by the amount of the dynamic pressure of the local peripheral speed:

$$^{2}\ p_f = \frac{\rho}{2}\omega^2\ r_M^2$$

ω signifying the angular velocity about the axis of rotation and r_M the vertical distance of the respective test point from this axis of rotation.

In order to avoid the lengthy determination by calculation of r_M for the various control-surface positions and yawing angles, a simple auxiliary device was manufactured which permits a direct measurement of the distances with an accuracy of about ±0.5 mm. The device may be fastened directly to the shaft-connection piece of the model which is adjusted in accordance with the respective angle of attack and of yaw (see fig. 8)[3].

For the representation, the actual pressures prevailing on the rotating model were - like those of the model at rest - made dimensionless by division by the dynamic pressure of the undisturbed flow. Since due to the rotation at the location of the measurement the relative free-stream velocity may, occasionally, be larger than the undisturbed free-stream velocity, it is understandable that the pressure-distribution curves for rotation may show partly higher positive pressures than $p/q = 1$.

2. Plotting of the Results, Definitions

Figure 9 shows the position of the measuring boreholes on the tail surfaces. In order to obtain clear diagrams, the pressure-distribution curves for horizontal and vertical tail surfaces were plotted separately (figs. 11 to 30). Positive pressures are plotted upward (right), negative pressures downward (left). Belonging to upper or lower side of the horizontal tail surfaces or, respectively, starboard or port side of the vertical tail surfaces is characterized by open or filled circles. Definition of the angles and the direction of rotation is also marked on the diagram to permit a better visualization.

In all tests the rotation took place clockwise, viewed from the pilot. The definition of the angles follows from figure 10. u signifies the peripheral speed of the wing tips ($\omega b/2$; b = span), so that

$$\frac{u}{v} = \frac{\omega b}{2v} = \lambda$$

---

[2]The centrifugal force still prevailing in the interior of the Fuhrmann gasket - since the distance of the test boring from the axis of rotation was very small compared to r_M - was neglected.

[3]This figure was totally indistinguishable in the only available copy of the original German document; therefore, it was not reproduced in the translated version.

V. DISCUSSION OF THE RESULTS

In figures 11 to 30 the results of the following measurements are plotted:

α for all measurements = 60°

ω for all measurements, clockwise, viewed from the pilot

All control surfaces on zero

$$\left.\begin{array}{l}\beta_S = +25^\circ \\ \beta_H = -20^\circ\end{array}\right\} \tau = 0 \left\{\begin{array}{l} v \sim 33\text{m/s};\ u = 0 \\ u/v \sim 0.3\end{array}\right.$$

$$\begin{array}{l}\tau = -10^\circ \\ \tau = +10^\circ\end{array} \quad \text{All control surfaces on zero} \left\{\begin{array}{l} v \sim 23\text{m/s};\ u = 0 \\ u/v \sim 0.6\end{array}\right.$$

As the most interesting result of the measurement one has to regard the fact that for all arrangements investigated in rotation the pressures on the vertical tail surfaces have the effect of originating a force in the direction of the rotation. For the investigated angle of attack of 60° the vertical tail surfaces have, therefore, due to the interference, not a damping, but on the contrary, an excitation effect. The reason can be seen from the measuring results. The vertical tail surfaces lie completely in the region of the separated flow of the horizontal-tail-surface suction side. Due to the additional component of the free-stream velocity caused by the rotation the direction of the oncoming flow is not in the symmetry plane of the horizontal tail surfaces. The negative pressures on the suction side and the positive pressures on the pressure side always lie higher on the leading than on the trailing wing. See for instance figures 11 and 13. Figure 11 shows the pressure distribution for $\tau = 0$, all control surfaces in zero position $\omega = 0$, and figure 13 the pressure distribution for the same position with rotation ($u/v \sim 0.3$). Without rotation the negative pressures lie on the average at 0.7 of the dynamic pressure, with rotation for the leading wing at about 0.85, for the trailing wing on the average at 0.55 of the dynamic pressure of the undisturbed flow. The vertical tail surfaces lie in this field of pressure. As one can see from figure 14, the negative pressures on the port side of the vertical tail surfaces are about 0.9 q, on the starboard side about 0.6 q, corresponding to the respective negative pressures of the horizontal-tail-surface section next to the fuselage. (In strength analyses, too, the different impingement of the flow on the horizontal tail surfaces should be taken into consideration).

Thus the flow at the horizontal tail surfaces is decisive for the pressure field surrounding the vertical tail surfaces in case the vertical tail surfaces are shielded by the horizontal tail surfaces. Rudder deflections, as shown in figure 18, are almost without effect. The curves of the pressure distribution for this case do not differ essentially from those represented in figure 14 (without rudder deflection). Only on the lowest part of the rudder, where it lies underneath the elevator, the larger negative pressures exist on the starboard side, and the port side still shows positive pressures toward the fuselage so that this part of the surface has a damping effect. Hence one can see the favorable effect of an upward shift of the horizontal tail surfaces. A larger part of the vertical tail surfaces is by this measure protected from interference and serves then for production of damping moments.

According to what has been said so far the forces on the horizontal tail surfaces also yield a rolling moment acting in the sense of rotation, thus having an excitation effect.

A downward elevator deflection produces, as is to be expected, a slightly more uniform positive-pressure area on the pressure side of the horizontal tail surfaces; the conditions on the suction side and the vertical tail surfaces, however, are hardly affected by it.

The flow at the tail surfaces is only slightly altered by positive or negative yawing angles. The interference effect of the fuselage on the region of the horizontal tail surfaces near the fuselage is significant for a positive yawing angle only. Figure 29 shows how on the section of the horizontal tail surfaces near the fuselage (starboard side) negative pressures still appear even on the front half of the pressure side, in contrast to figure 25 (negative yawing angle) where the pressures show positive amounts of 0.4 q to the end of the elevator. (A subsequent control measurement confirmed the pressure distribution of the section near the fuselage represented in figs. 25 and 29.)

For the vertical tail surfaces, the influence of the rotation predominates over that of the yawing angle. For negative yawing angle (without rotation) the negative pressures on the left side and for positive yawing angle the negative pressures on the right side become larger than on the respective opposite side - again corresponding to the pressure distribution over the horizontal tail surfaces. Only for the uppermost section of the vertical tail surfaces are the conditions always reversed. Probably here already a relief of the negative pressure takes place.

The measurements with yawing angles could be performed only for higher values of u/v, since for $\tau = \pm 10^{\circ}$ the autorotational velocity of the model already assumed too great values and the existing suspension device did not permit braking. Clockwise autorotation occurred for a positive yawing angle. It is started by the wing alone since, as the

tests show at the beginning of the motion, the resultant air forces on the tail surfaces (horizontal as well as vertical tail surfaces) take effect against the starting rotation. Once the rotation is established the sign of the air forces affecting the tail surfaces is reversed and they yield now a contribution promoting the rotation.

Finally, the plotting of the pressures against the tail-surface areas was dealt with as if rudder and fin would form an uninterrupted area. Actually the rudder slot on the model was vanishingly small so that no noteworthy pressure balance could take place. One can see that from the fact that all pressure distributions over the various sections of the horizontal tail surfaces show only a slight recess in the curve between the last test point on the fin and the first test point on the elevator.

VI. INDICATION OF FURTHER MEASUREMENTS TO BE PERFORMED WITH A TEST ARRANGEMENT ALREADY BEING DEVELOPED

The new tests with the model of the M 31 are to be continued for various smaller angles of attack, also for the further case of the axis of rotation not passing through the center of gravity. Furthermore, it is intended to investigate other forms of tail surfaces and other positions of the horizontal tail surfaces and to perform measurements on the vertical tail surfaces with the horizontal tail surfaces taken off, in order to obtain more data for the study of flow phenomena at the tail surfaces in spin.

A new test arrangement will be required since the apparatus used for the investigations described here which actually was destined only for measurements with lighter models proved too weak for the case. Besides this new test arrangement a new type of pressure-transfer device shall be used in order to avoid the difficulties impeding the simultaneous transfer of a multitude of pressures. With that apparatus it will be possible to conduct 26 pressure lines coming from the model one after another to only one gasket without interruption of the steady rotary motion. This device is described in a separate report by W. Mautz under the title, "Eine neuartige Druckumschaltvorrichtung fur Druckmessungen an rotierenden Systemen" (A new type of pressure switch for pressure measurements on rotating systems).

VII. SUMMARY

The results of the first pressure-distribution measurements on the tail surfaces of a rotating model of the BFW - M 31 were reported. The measurements which were made without rotation for an angle of attack of

60° showed as the most important result that for this angle of attack the vertical tail surfaces are completely shielded. In the case of rotation due to the pressure conditions at the horizontal tail surfaces an excitation moment is produced, independent of the rudder angle and the angle of yaw. The influences of rudder and yawing angles were discussed and the results of all pressure distribution measurements represented on graphs.

The test arrangement used was described and a new one which is being developed pointed out. The intended enlarged test program was briefly reported.

Translated by Mary L. Mahler
National Advisory Committee
for Aeronautics

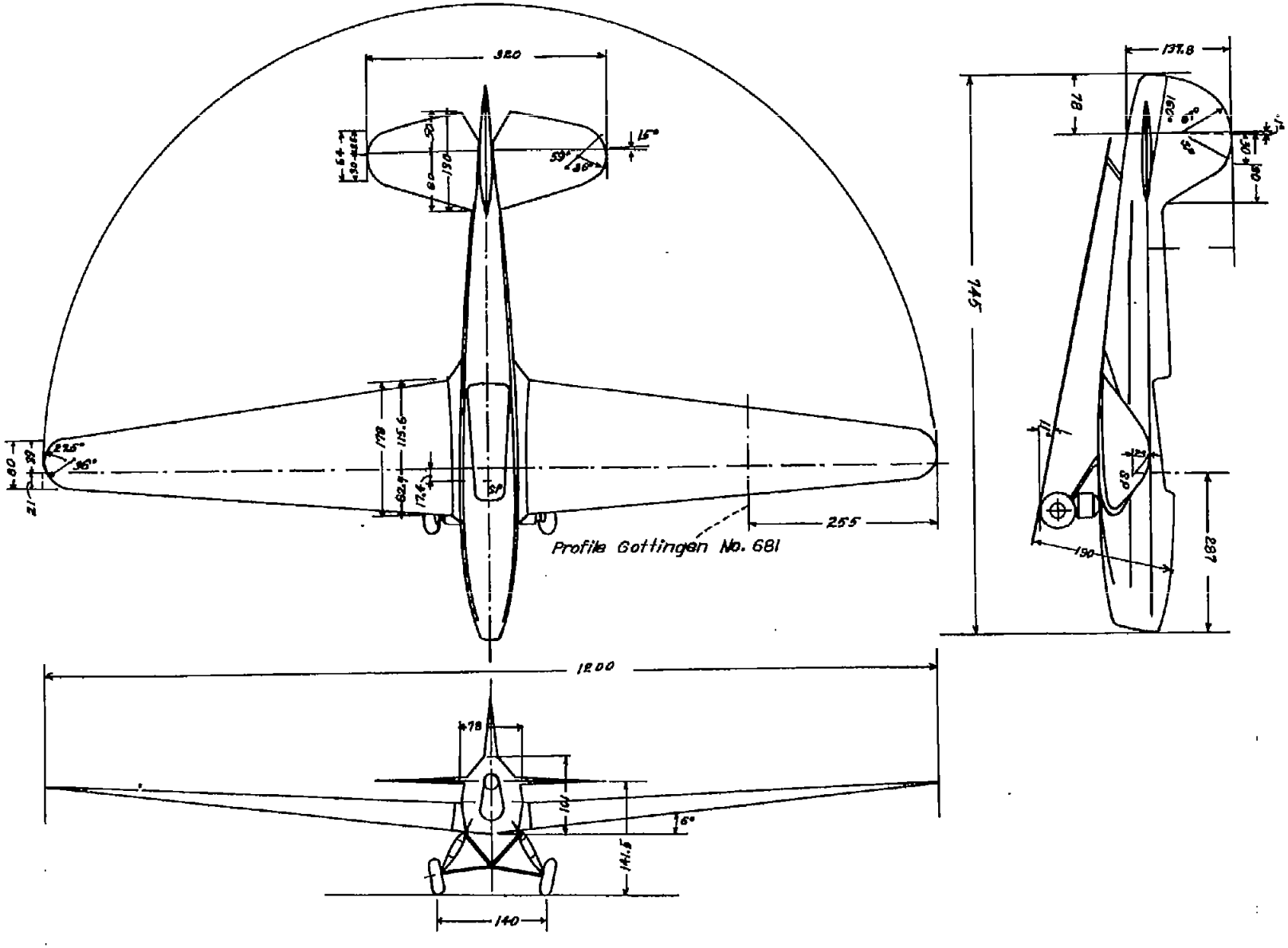

Figure 1.- Survey diagram of the model of the BFW - M 31.

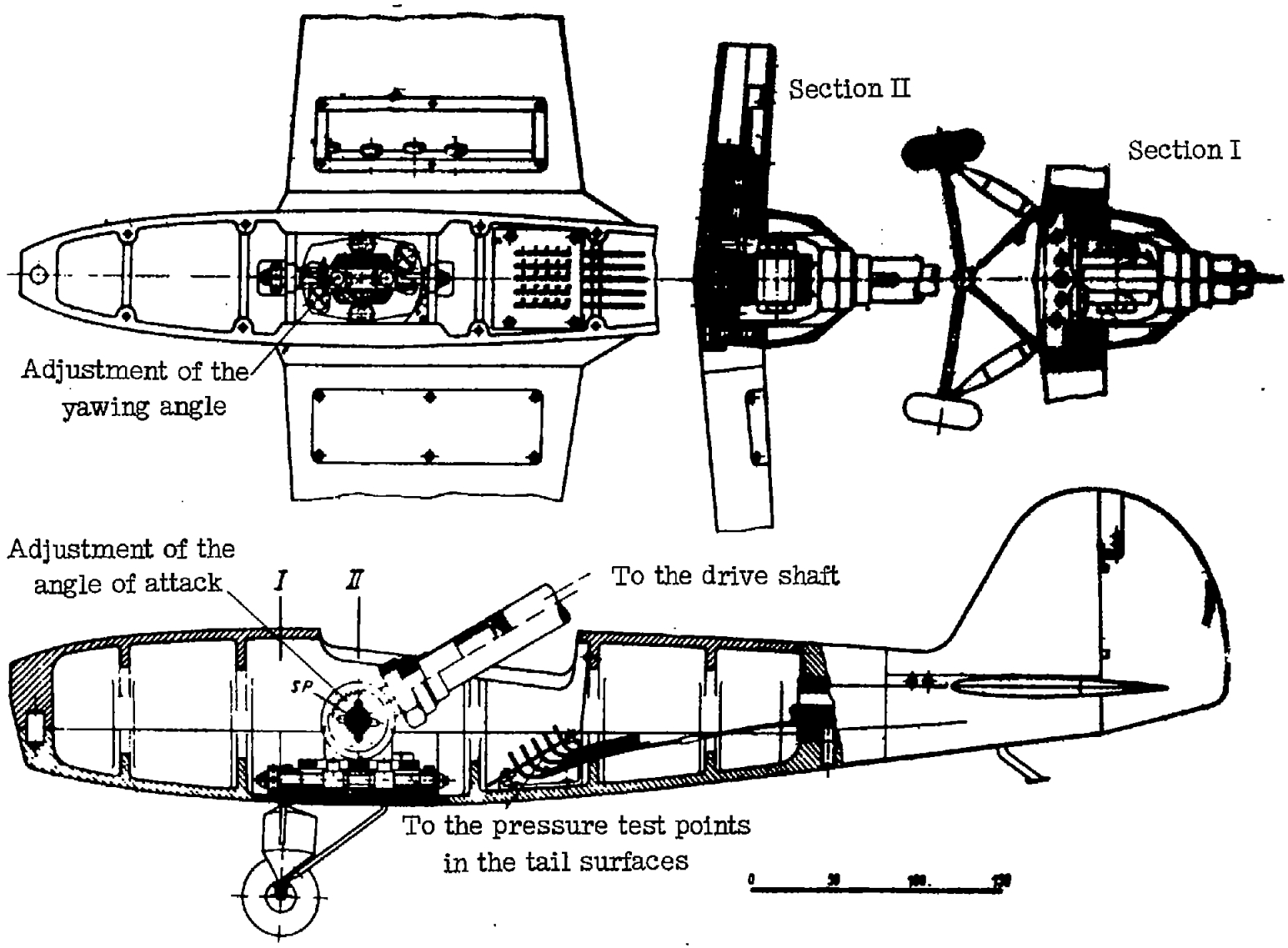

Figure 2.- Details of the model design.

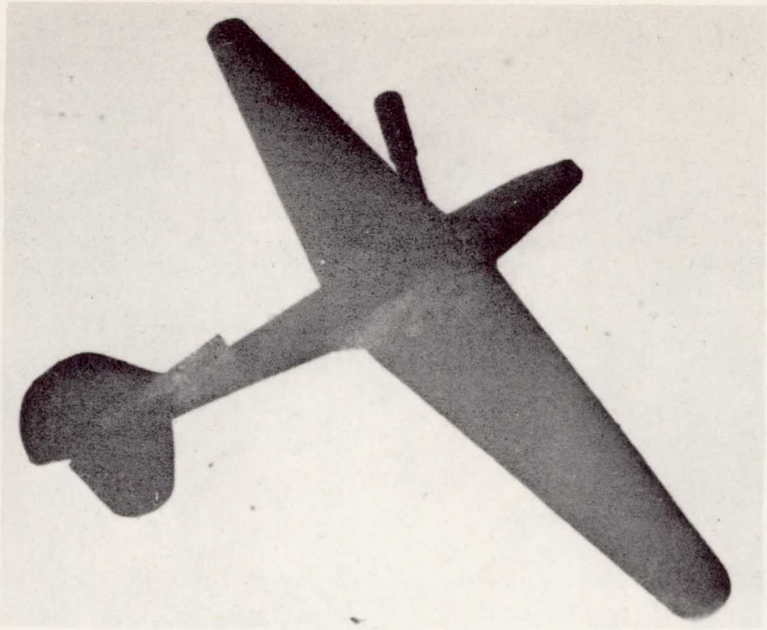

Figure 3.

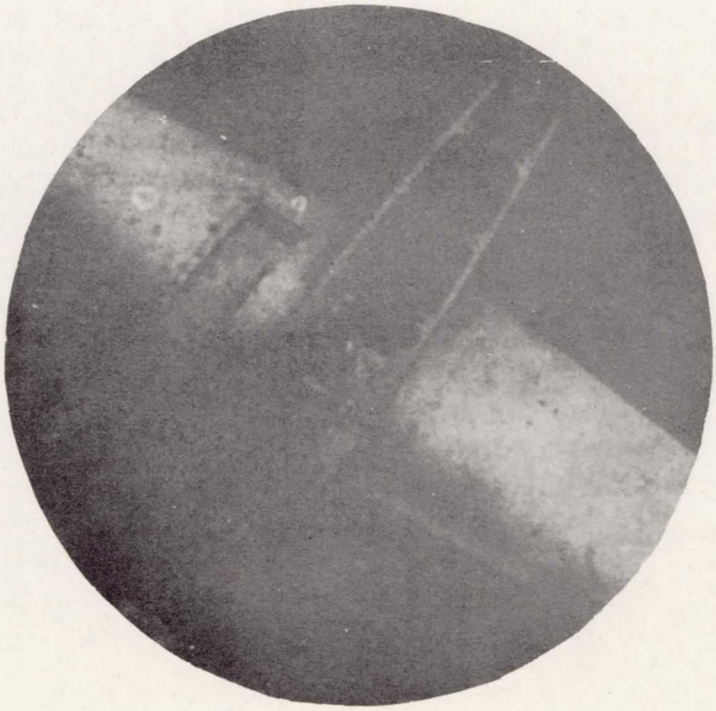

Figure 4.

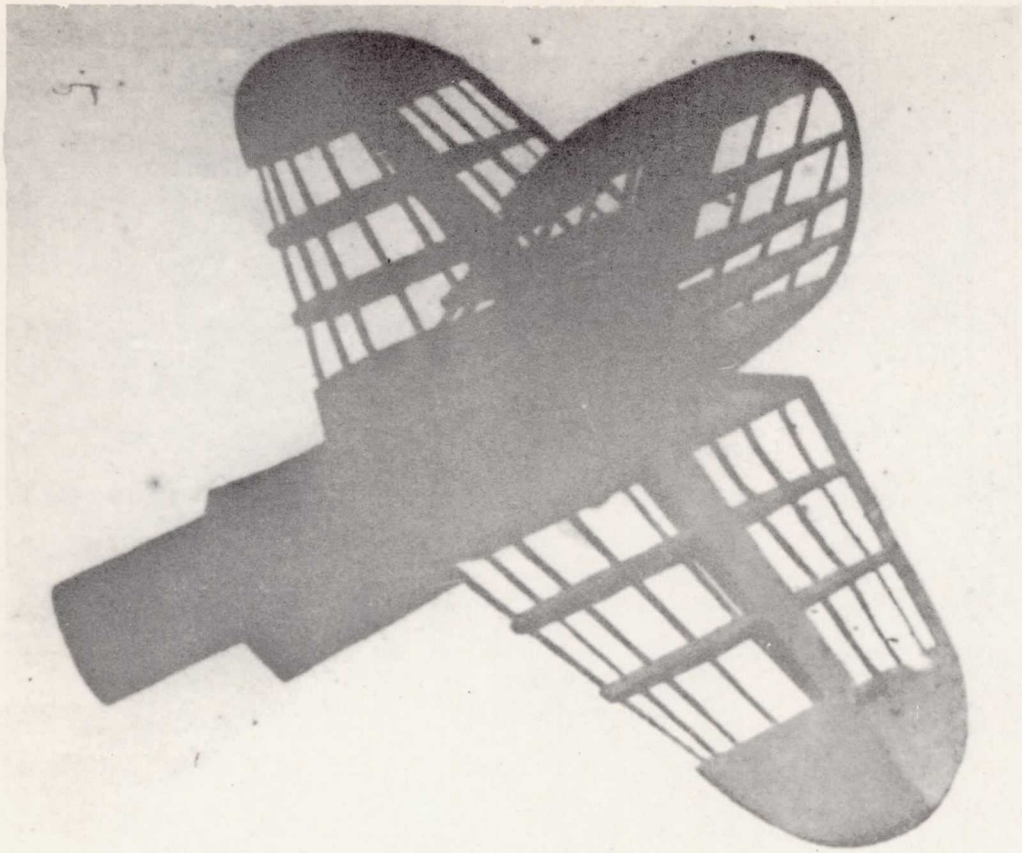

Figure 5.- Interchangeable fuselage end with the framework of the tail-surface areas.

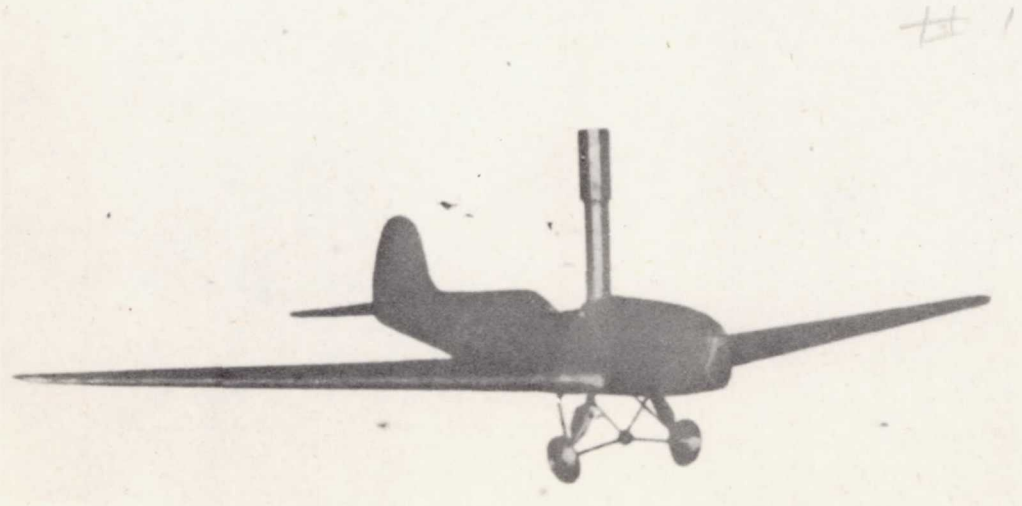

Figure 6.- View of the model with the shaft-connecting piece.

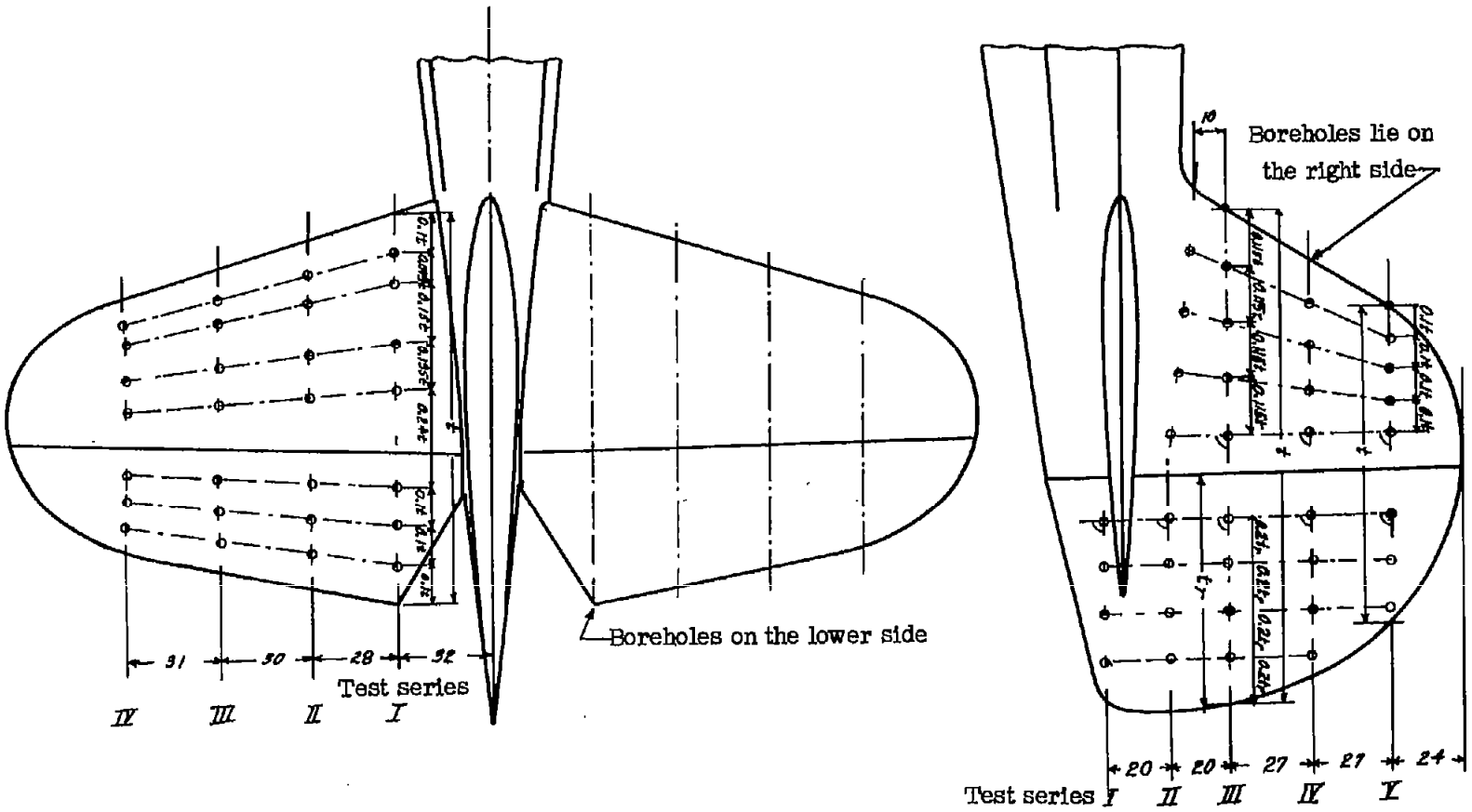

Figure 9.- Arrangement of the test boreholes on the tail surfaces.

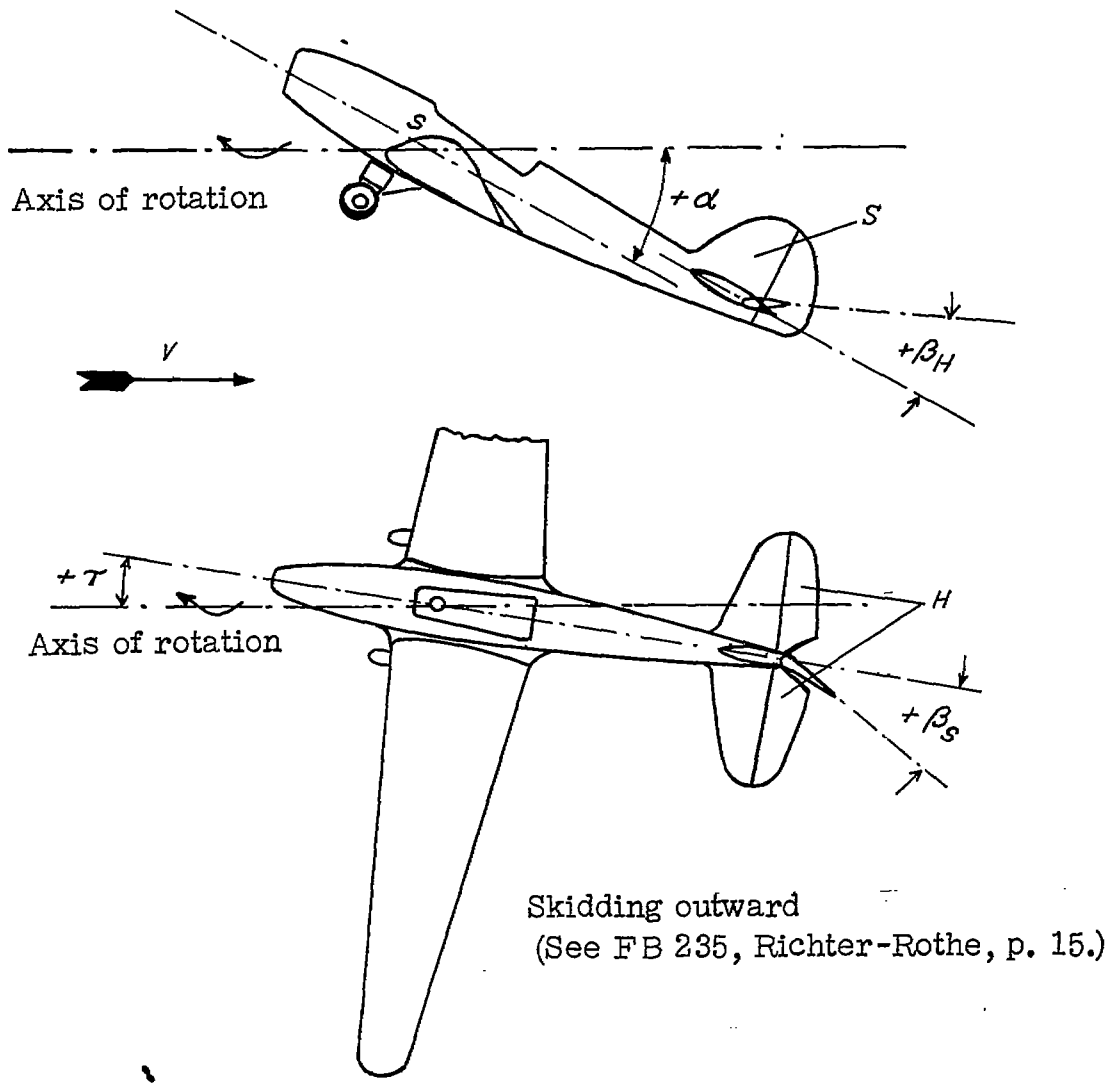

Figure 10.- Sketch indicating definitions.

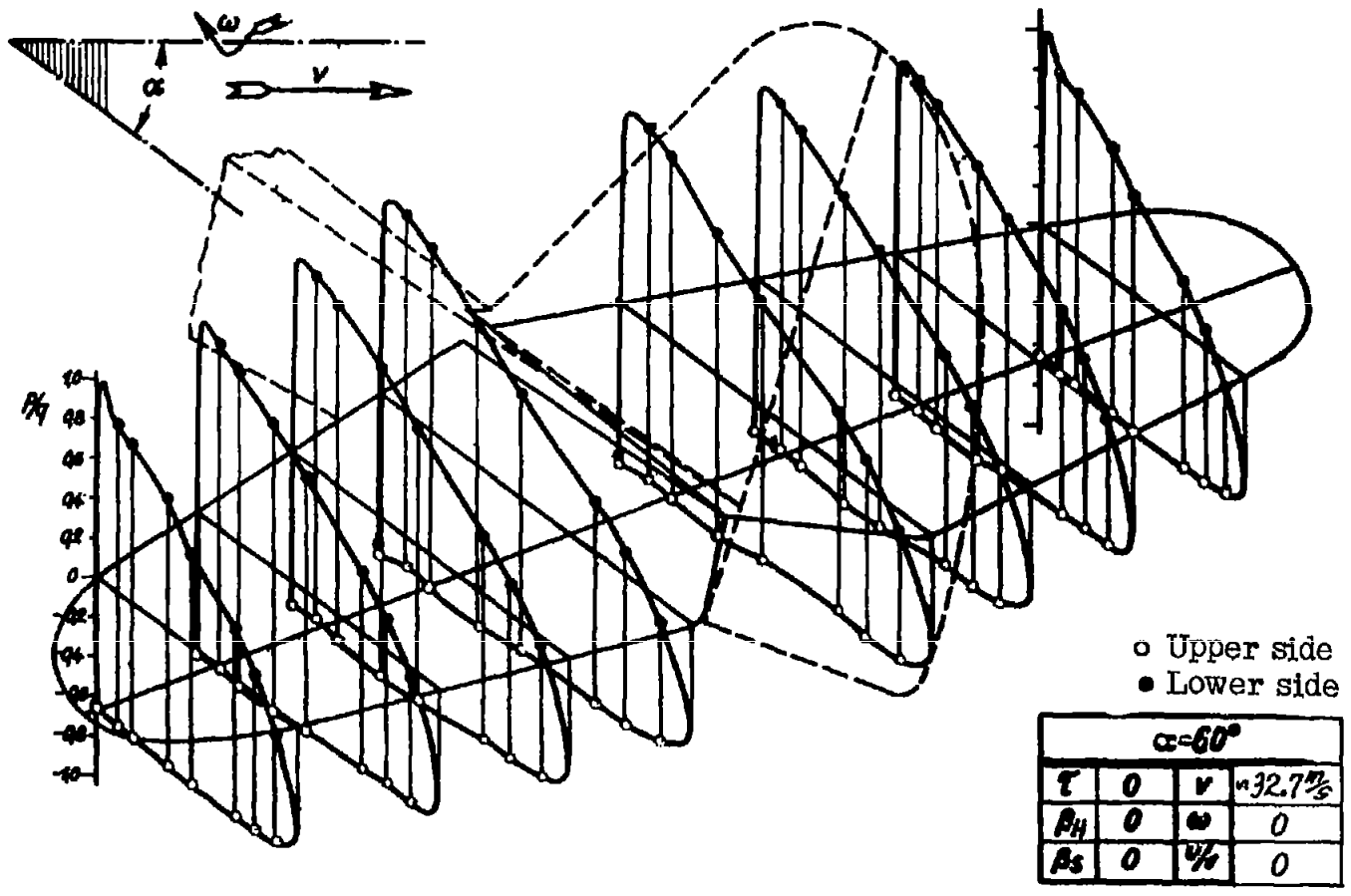
α
v
p/q
1.0
0.8
0.6
0.4
0.2
0
-0.2
-0.4
-0.6
-0.8
-1.0
o Upper side
• Lower side
α=60°
τ 0 v ≈32.7 m/s
β_H 0 ω 0
β_S 0 ψ 0

Figure 11.

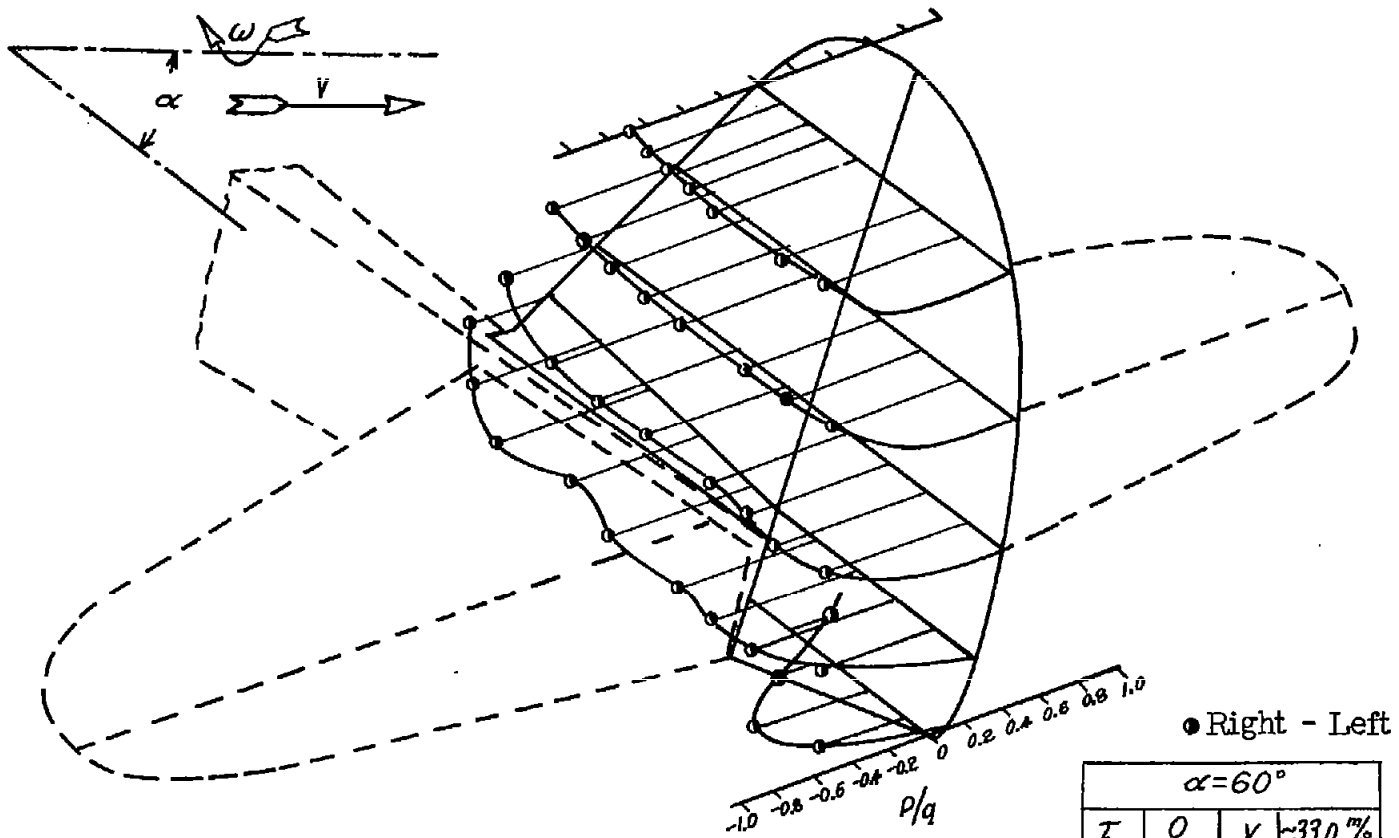

$\alpha = 60°$			
τ	0	V	-33.0 m/s
β_H	0	ω	0
β_S	0	u/v	0

Figure 12.

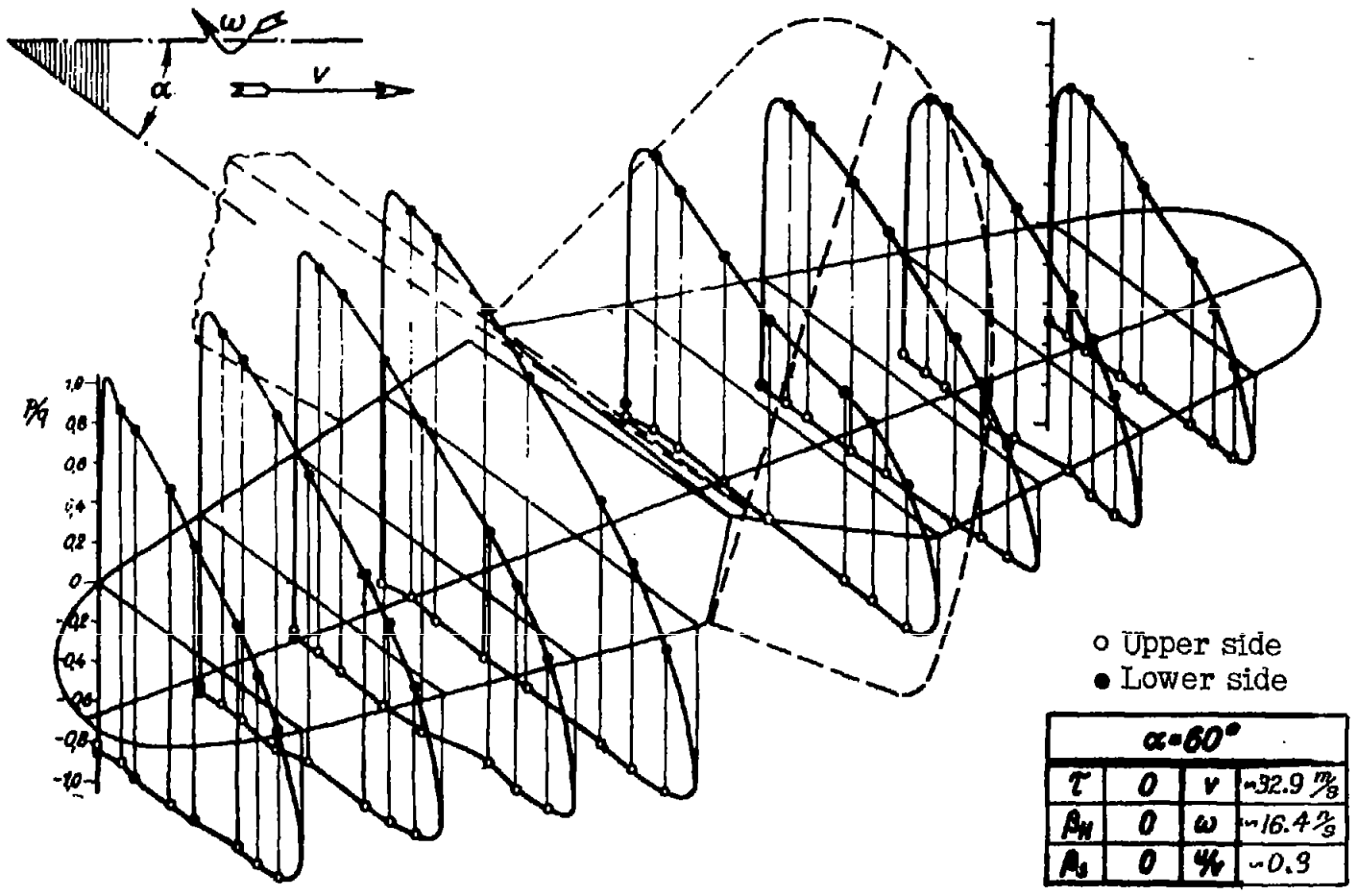
ω
α
v
P/q
1.0
0.8
0.6
0.4
0.2
0
-0.2
-0.4
-0.6
-0.8
-1.0
o Upper side
• Lower side
α=60°
τ 0 v ~32.9 m/s
β_H 0 ω ~16.4 °/s
A_s 0 ψ ~0.3

Figure 13.

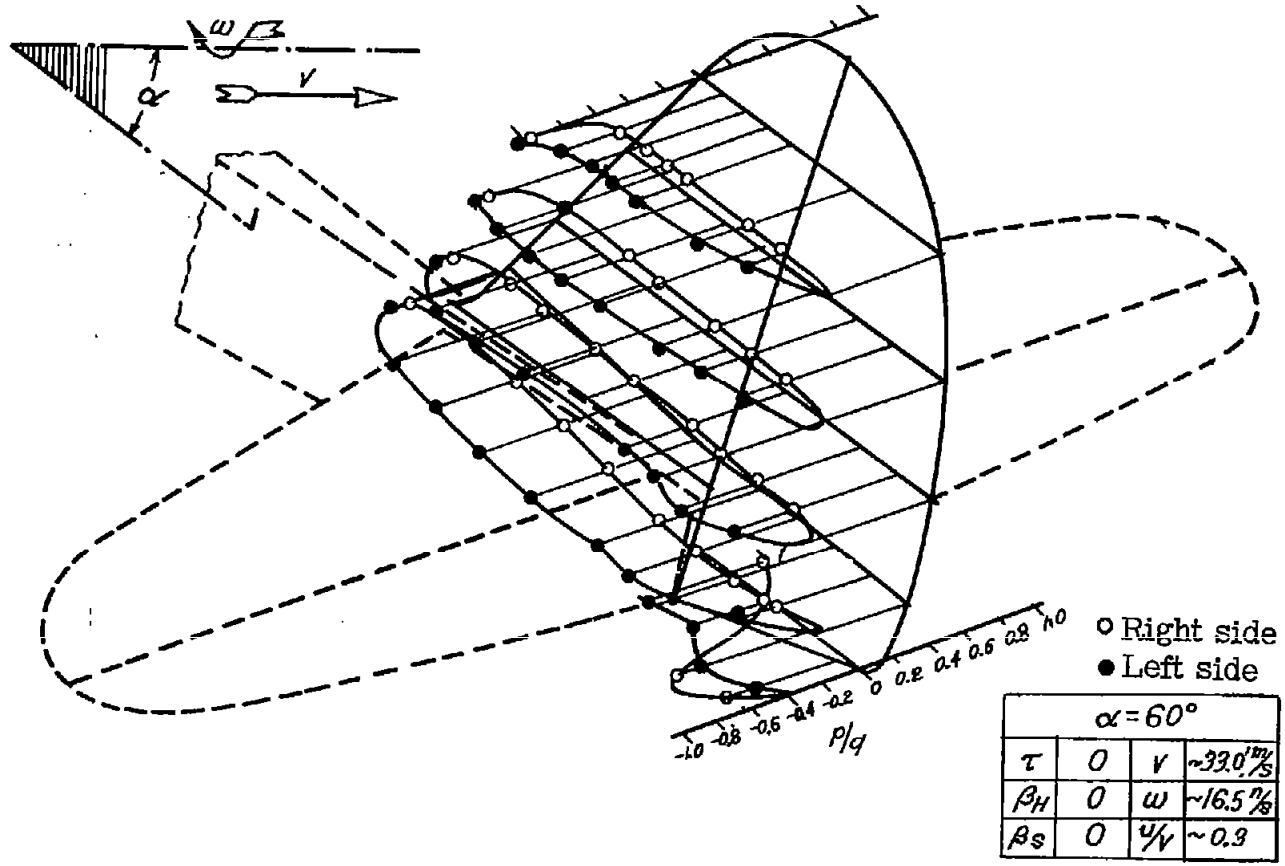
ω
β
α
V
-1.0 -0.8 -0.6 -0.4 -0.2 0 0.2 0.4 0.6 0.8 1.0
P/q
○ Right side
● Left side
α = 60°
τ 0 V ~33.0 m/s
βH 0 ω ~16.5 m/s
βs 0 u/V ~0.3

Figure 14.

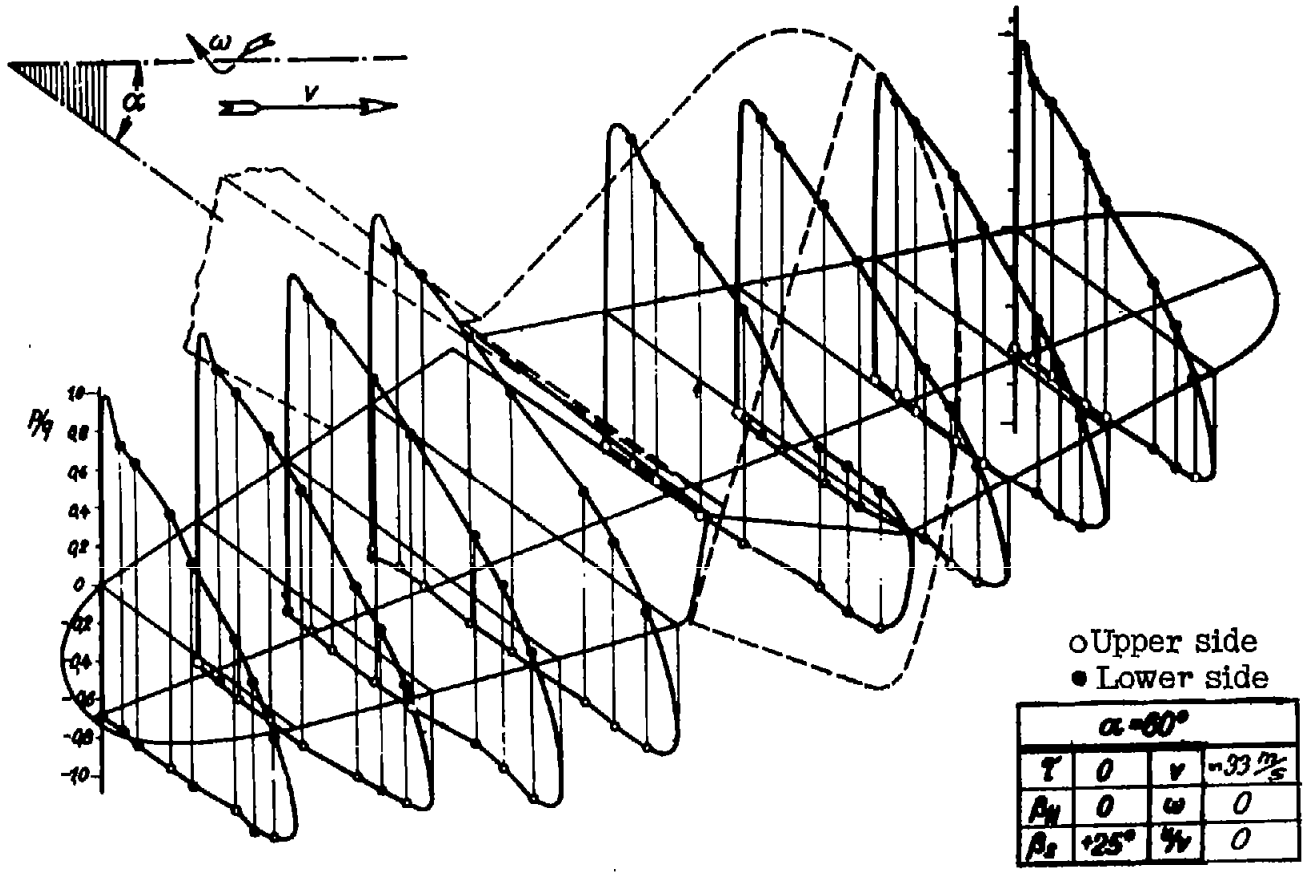
ω
α
v
p/q
1.0
0.8
0.6
0.4
0.2
0
-0.2
-0.4
-0.6
-0.8
-1.0
o Upper side
• Lower side
α = 60°
τ 0 v ≈33 m/s
βy 0 ω 0
βs +25° ψ 0

Figure 15.

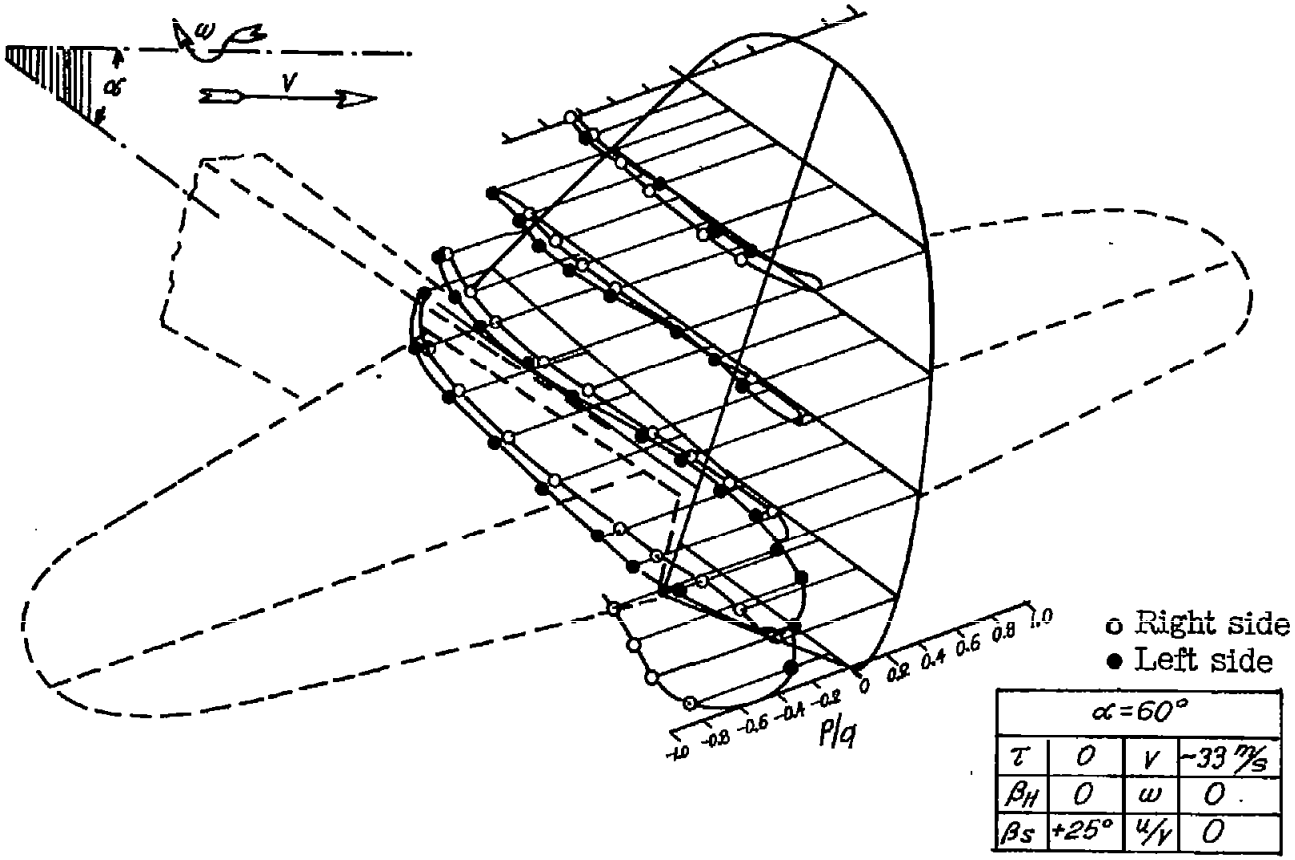
ω
α
V
-1.0
-0.8
-0.6
-0.4
-0.2
0
0.2
0.4
0.6
0.8
1.0
P/q
o Right side
● Left side
α = 60°
τ 0 V ~33 m/s
βH 0 ω 0
βs +25° u/V 0

Figure 16.

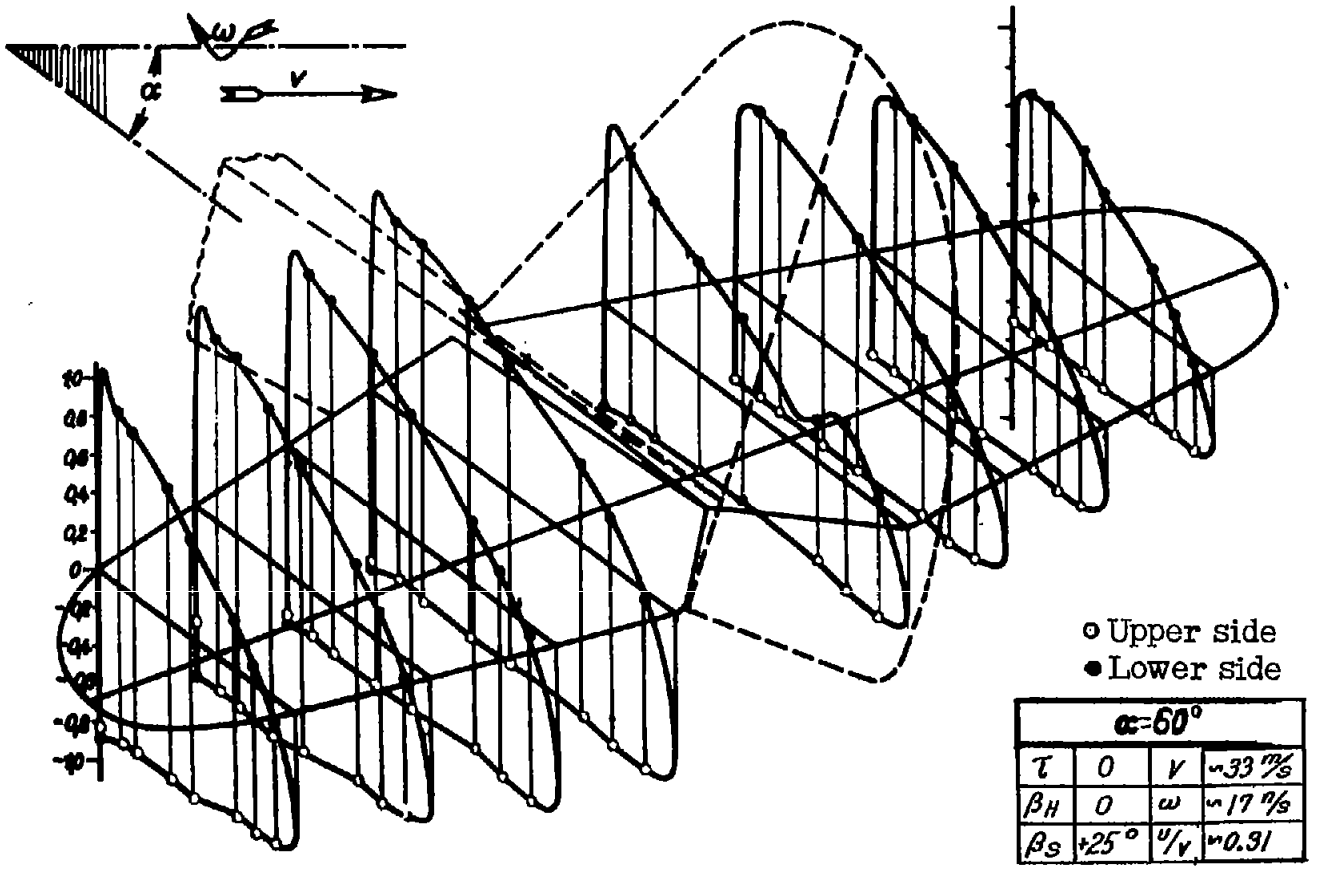
α
v
ω
1.0
0.8
0.6
0.4
0.2
0
-0.2
-0.4
-0.6
-0.8
-1.0
○ Upper side
● Lower side
α=60°
τ 0 v ~33 m/s
βH 0 ω ~17 °/s
βS +25° u/v ~0.31

Figure 17.

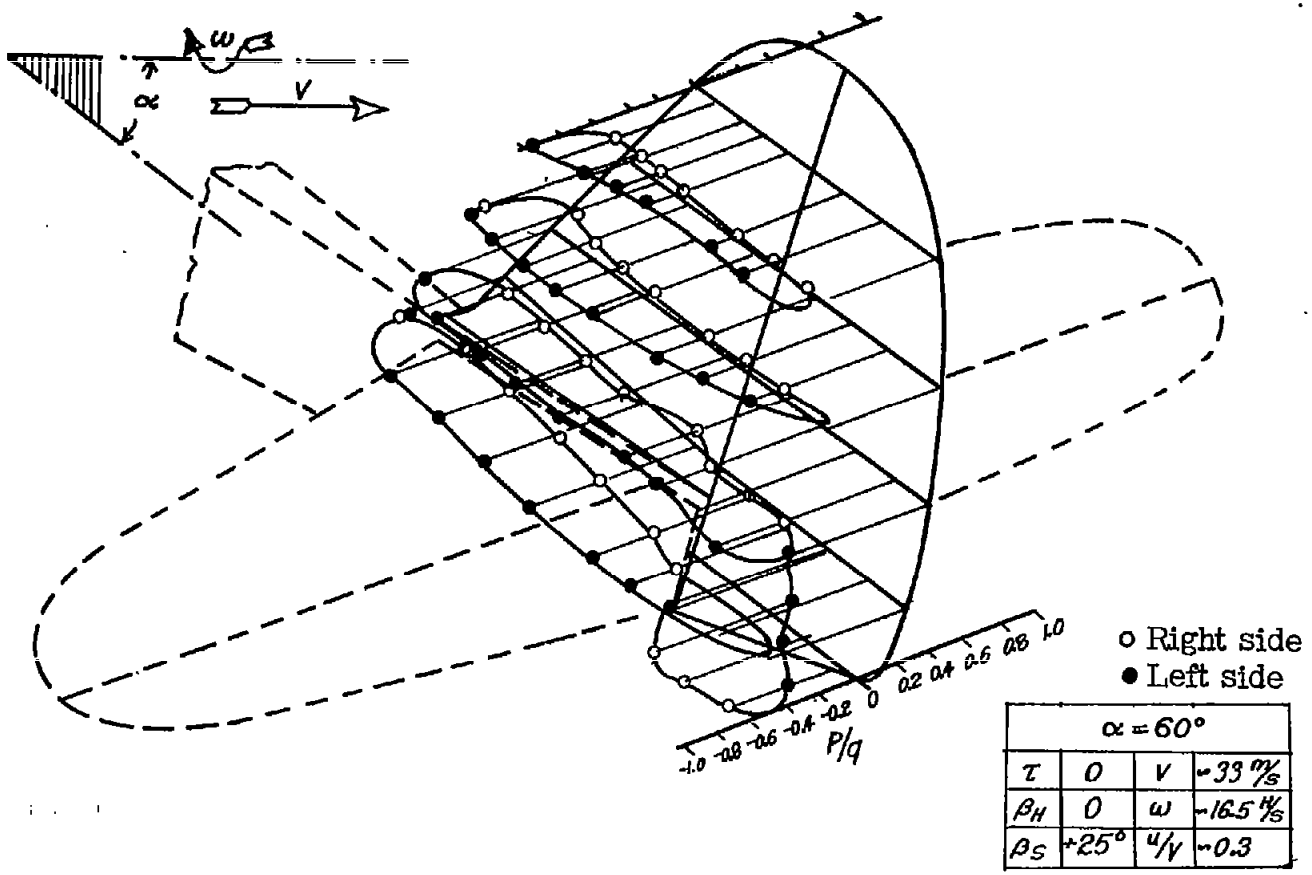
ω
β
α
V
-1.0 -0.8 -0.6 -0.4 -0.2 0 0.2 0.4 0.6 0.8 1.0
P/q
o Right side
● Left side
α = 60°
τ 0 V -33 m/s
β_H 0 ω -16.5 ft/s
β_S +25° u/V -0.3

Figure 18.

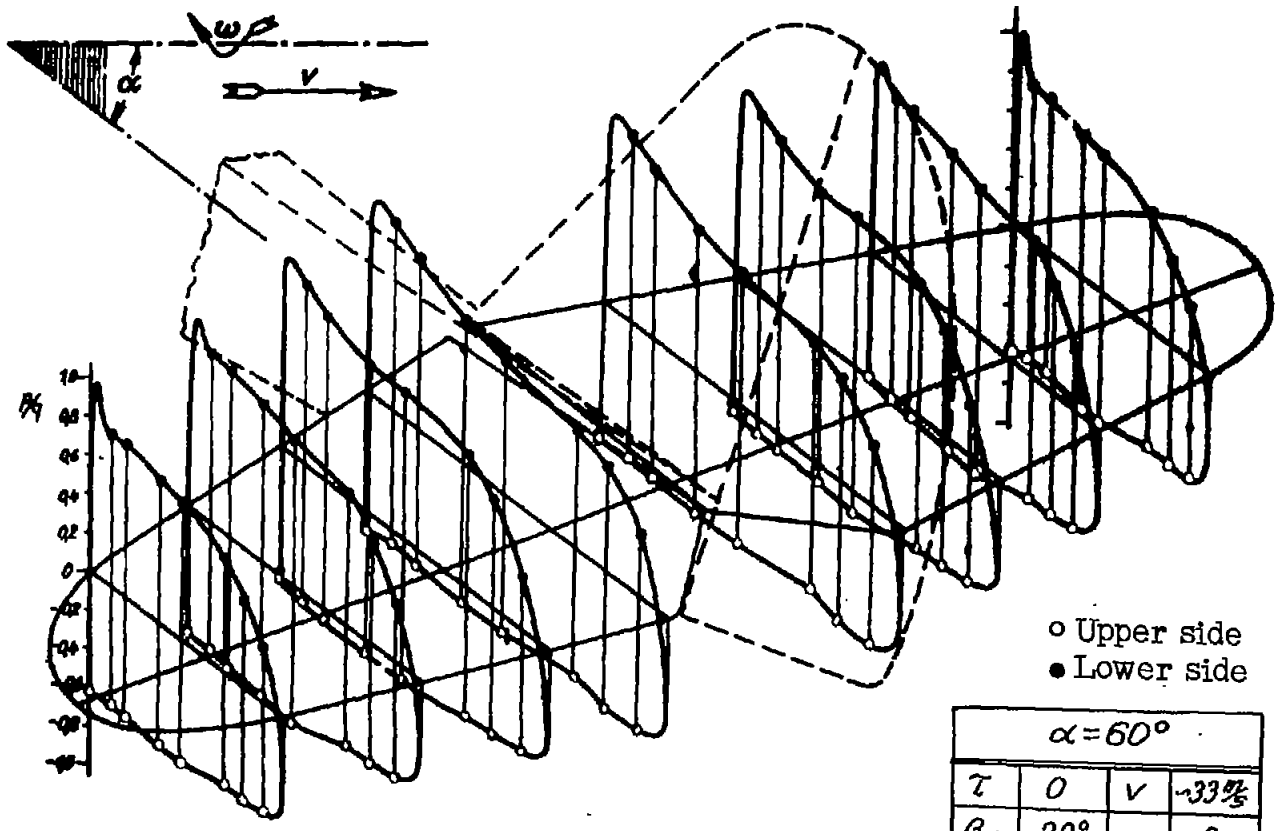

$\alpha = 60°$			
τ	0	v	~33 m/s
β_H	-20°	ω	0
β_S	0	u/v	0

Figure 19.

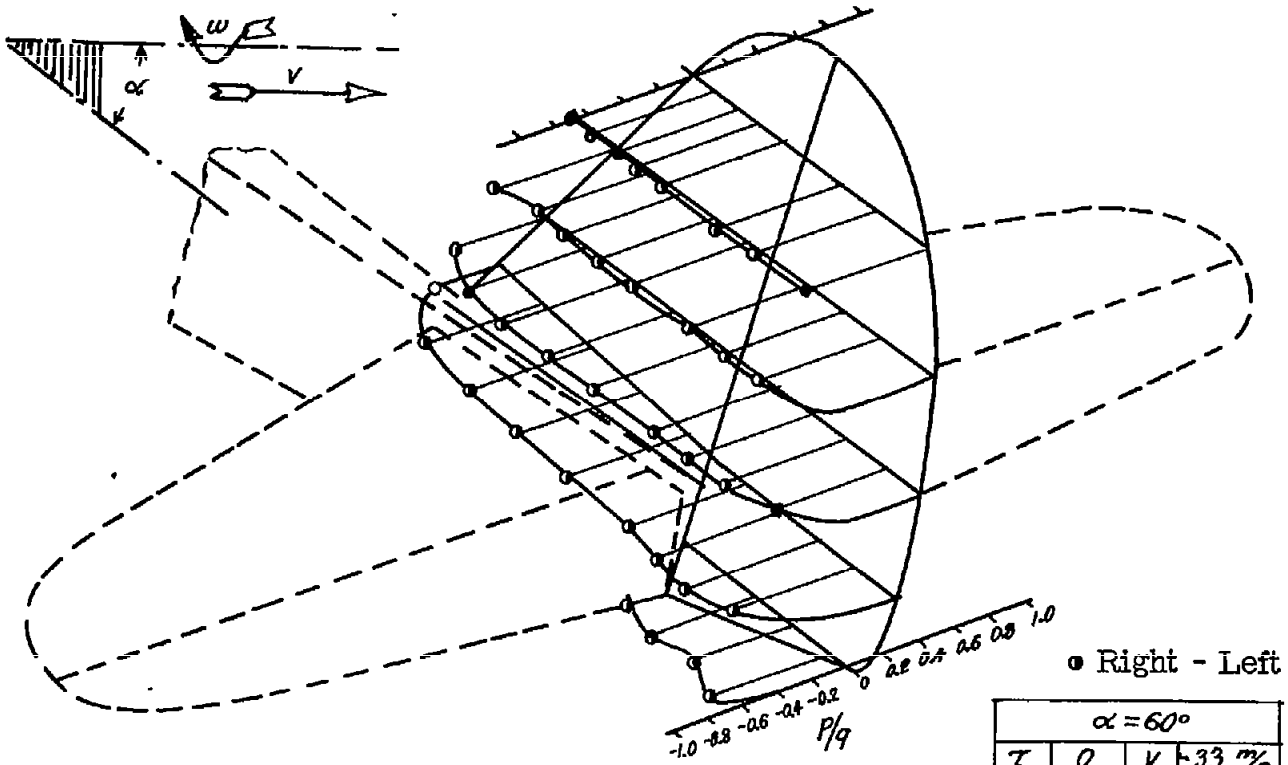

$\alpha = 60°$			
τ	0	V	33 m/s
β_H	-20°	ω	0
β_S	0	ψ/V	0

Figure 20.

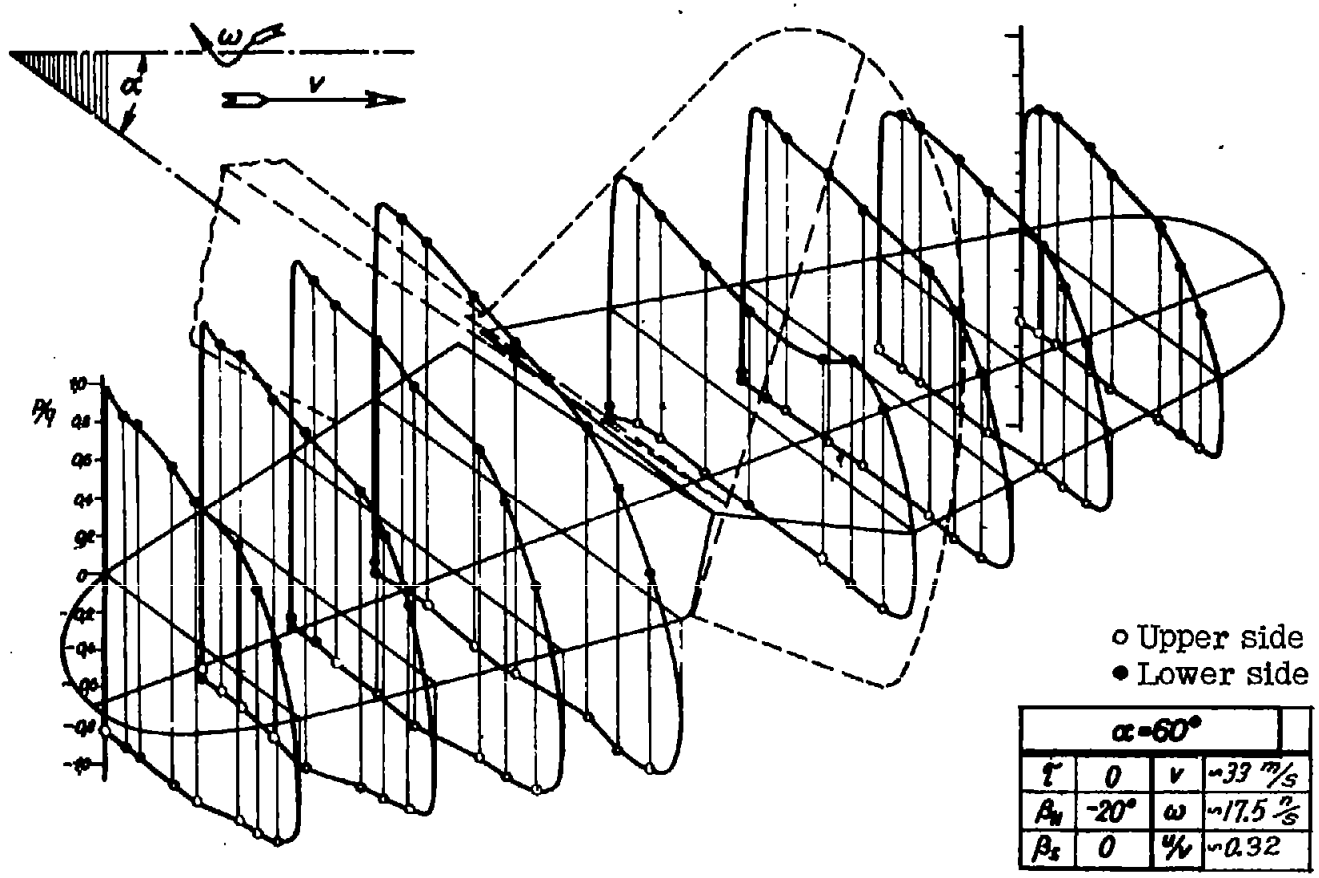
ω
α
v
p/q
o Upper side
• Lower side
α=60°
τ 0 v ~33 m/s
β_H -20° ω ~17.5 n/s
β_S 0 u/v ~0.32

Figure 21.

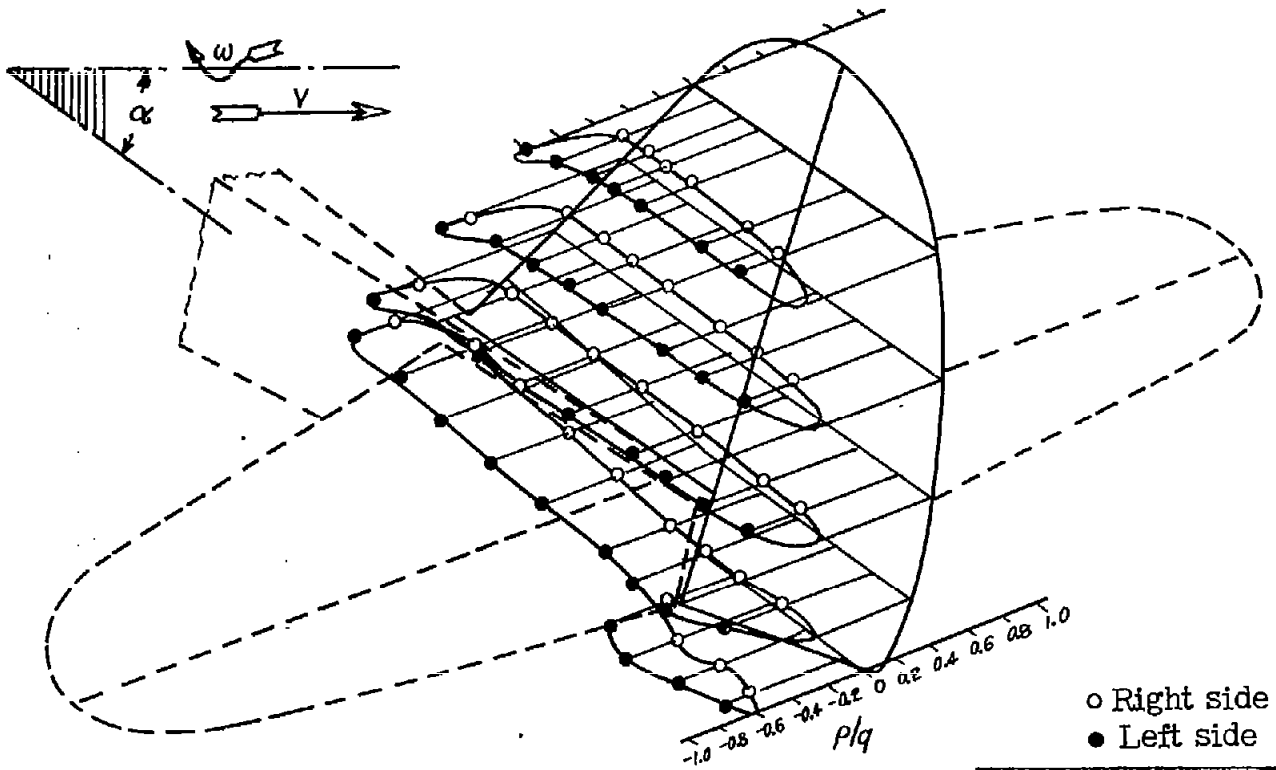

o Right side
● Left side

$\alpha = 60°$			
τ	0	V	~33 m/s
β_H	-20°	ω	~19 °/s
β_S	0	u/V	~0.34

Figure 22.

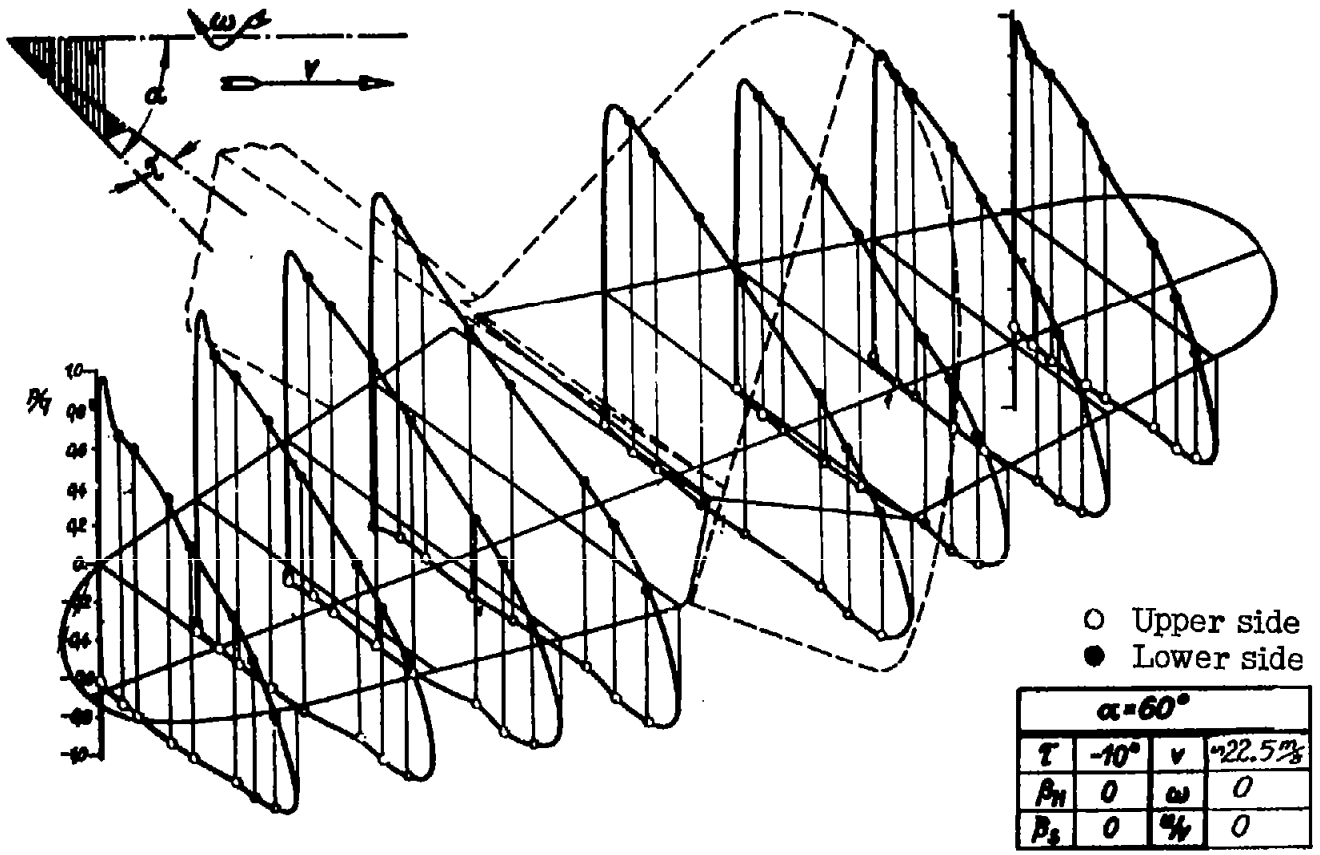
ω
v
α
P/q
1.0
0.8
0.6
0.4
0.2
0
-0.2
-0.4
-0.6
-0.8
-1.0
○ Upper side
● Lower side
α=60°
τ
-10°
v
~22.5 m/s
β_H
0
ω
0
β_S
0
u/v
0

Figure 23.

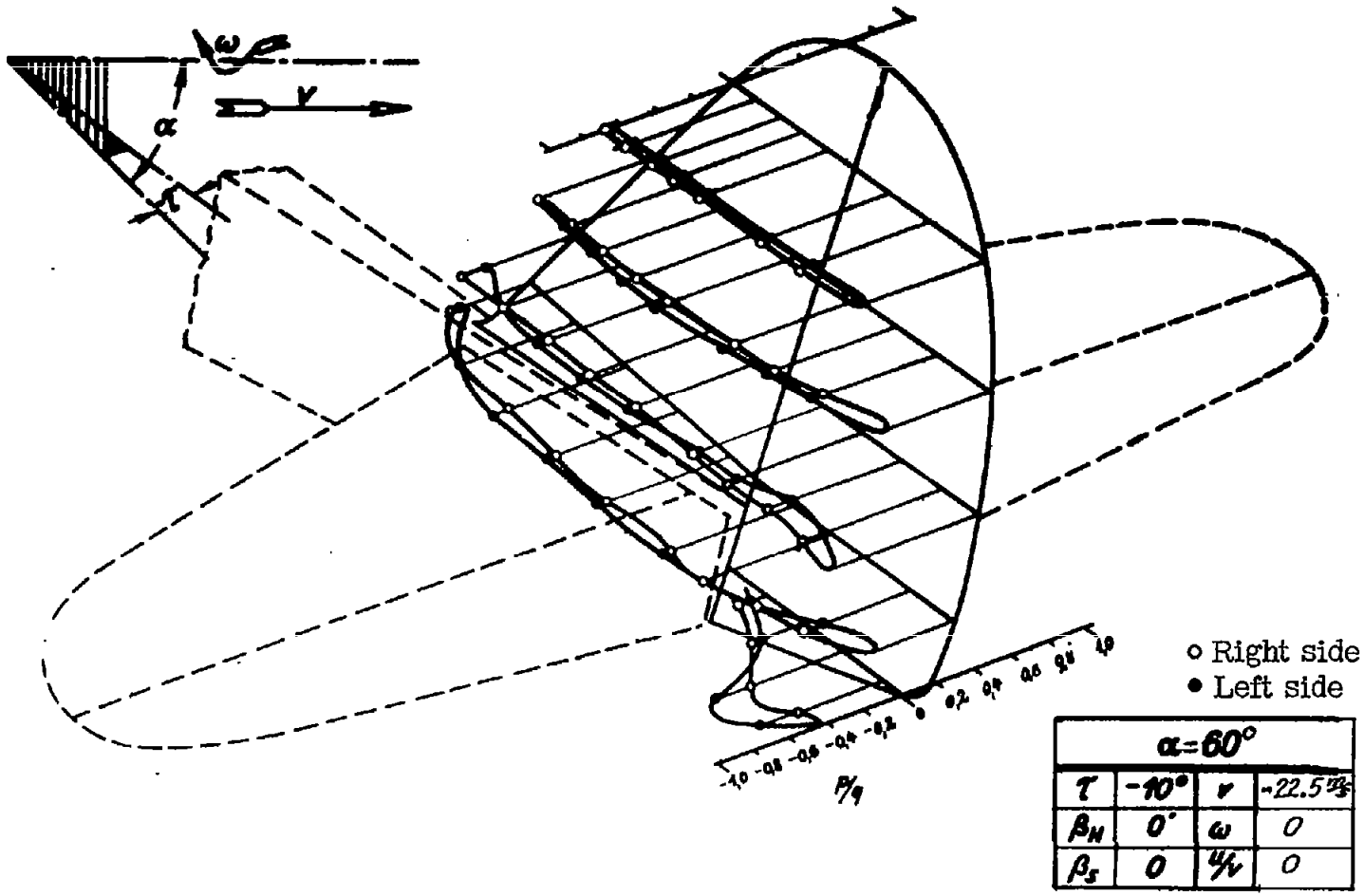

α=60°			
τ	-10°	v	-22.5 m/s
β_H	0°	ω	0
β_s	0	u/v	0

Figure 24.

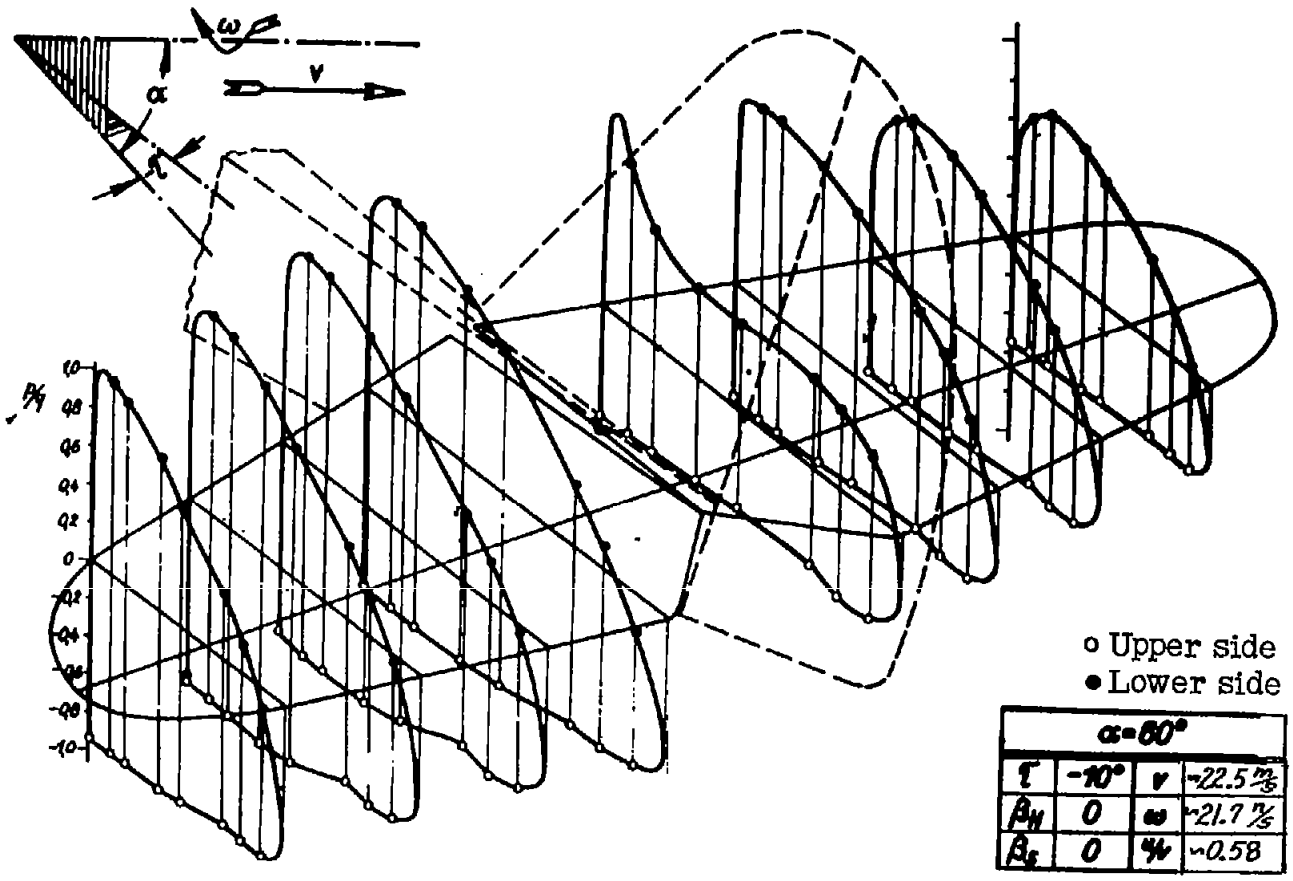
ω
v
α
τ
β_H
1.0
0.8
0.6
0.4
0.2
0
-0.2
-0.4
-0.6
-0.8
-1.0
o Upper side
• Lower side
α=60°
τ -10° v ~22.5 m/s
β_H 0 ω ~21.7 1/s
β_S 0 ω/v ~0.58

Figure 25.

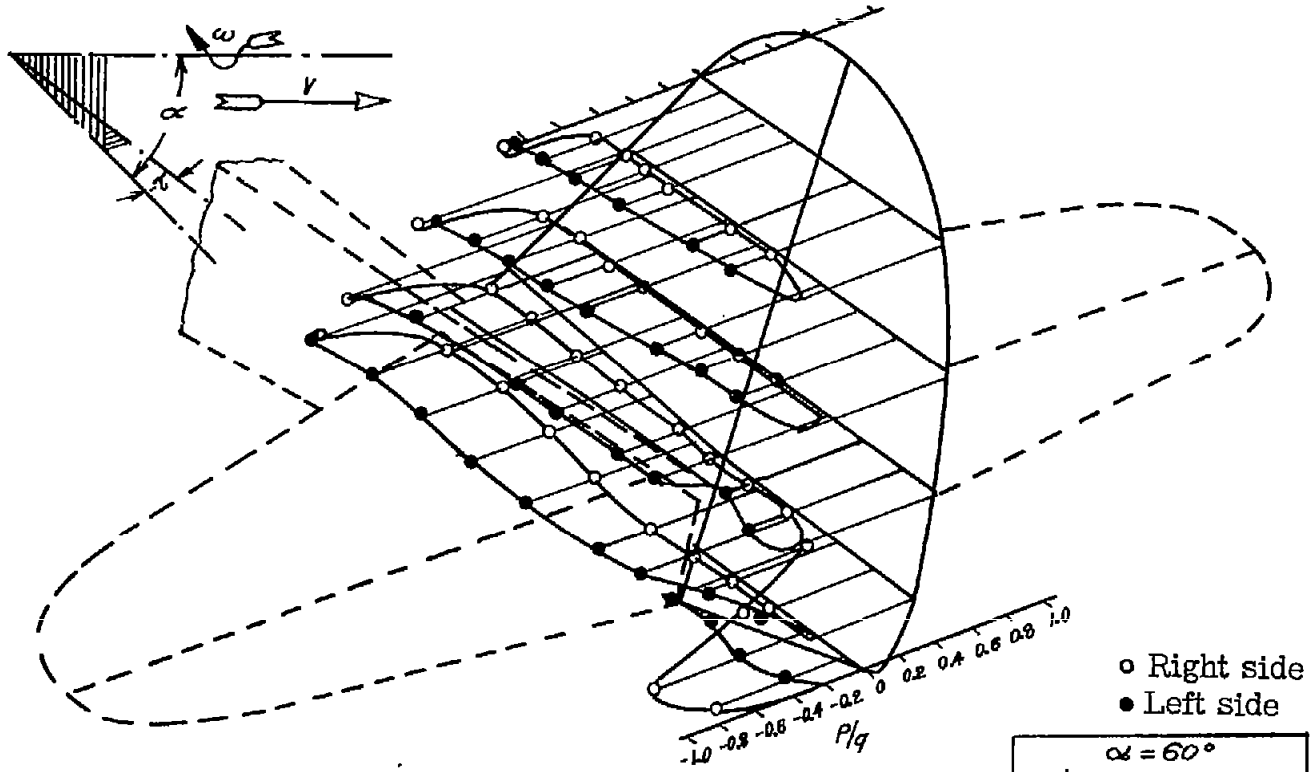

$\alpha = 60°$			
τ	$-10°$	V	-22.5 m/s
β_H	0	ω	-22.8 r/s
β_S	0	u/V	-0.58

Figure 26.

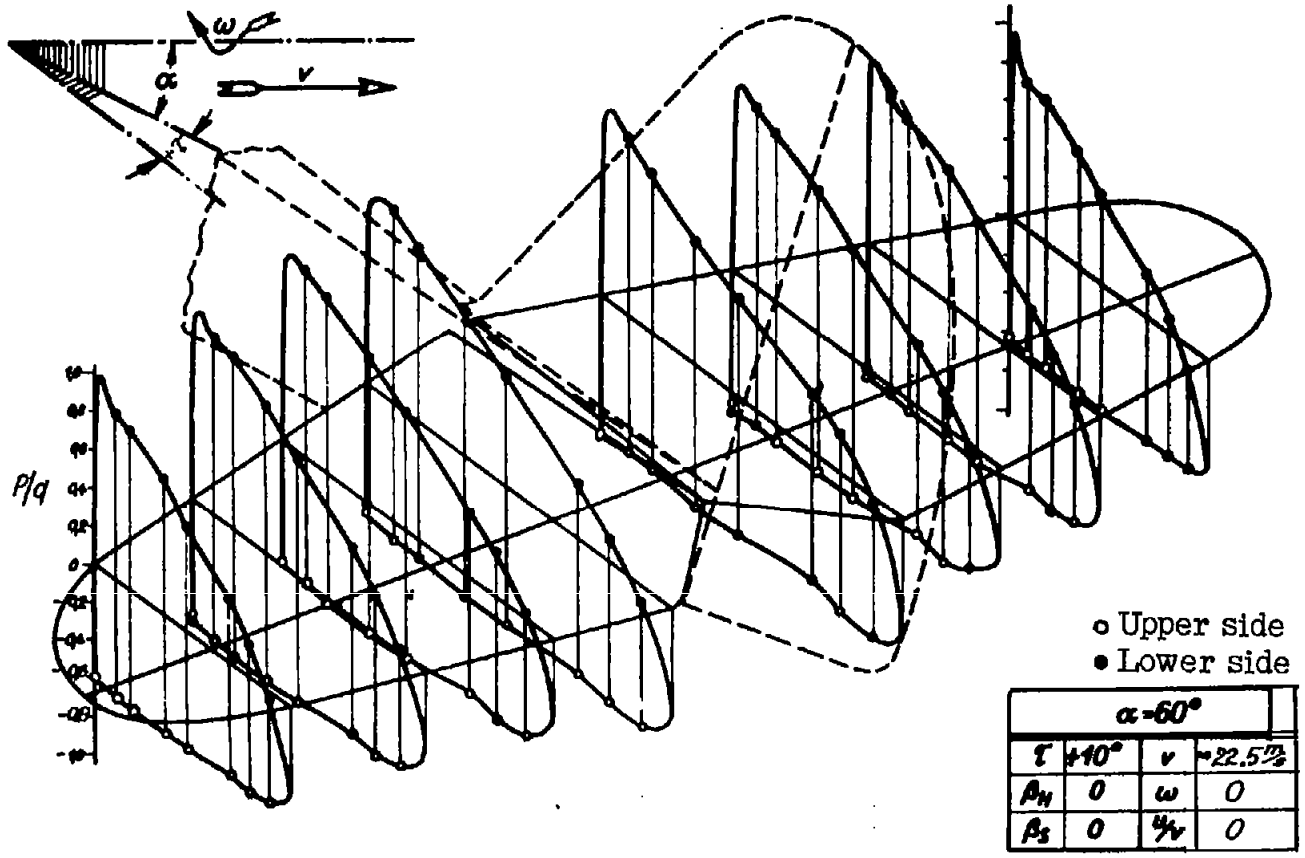

Figure 27.

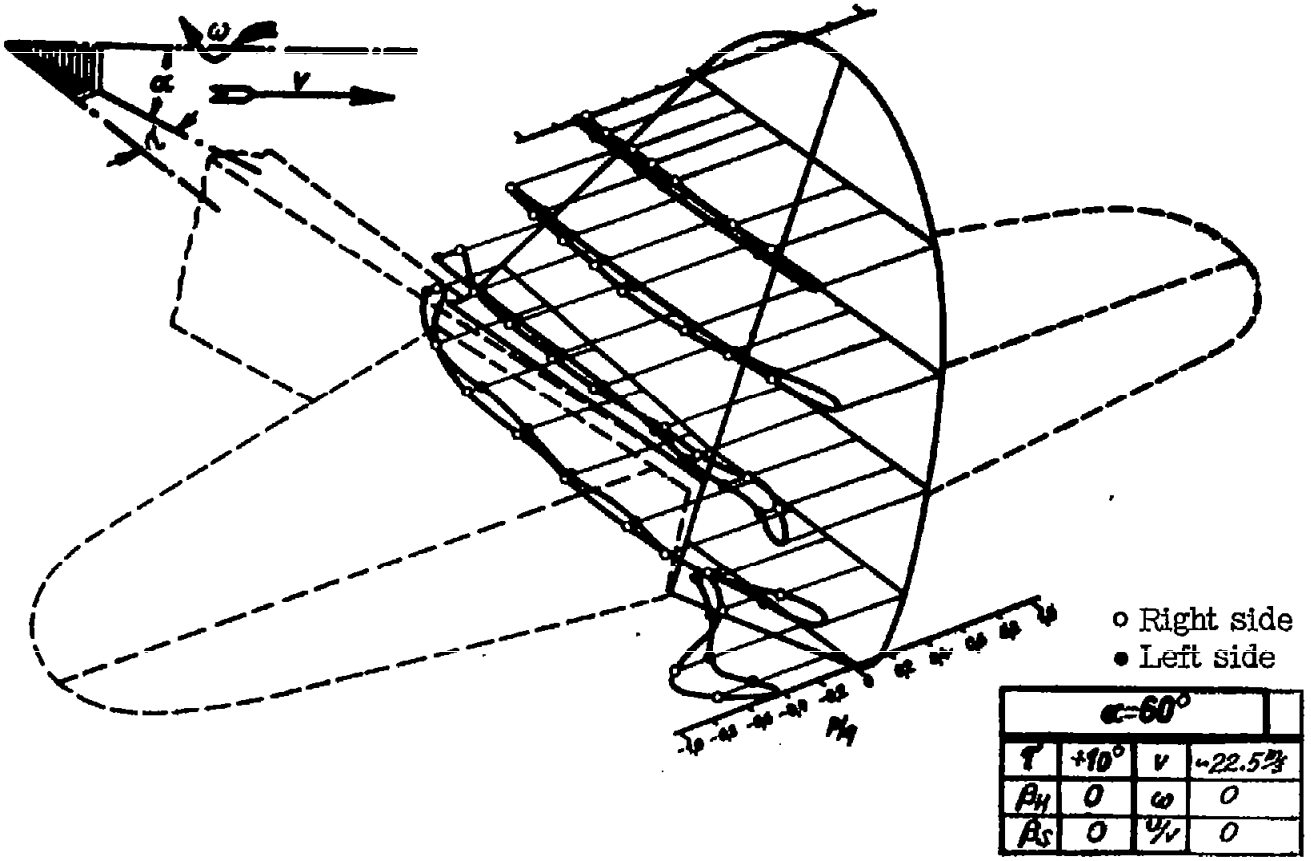

Figure 28.

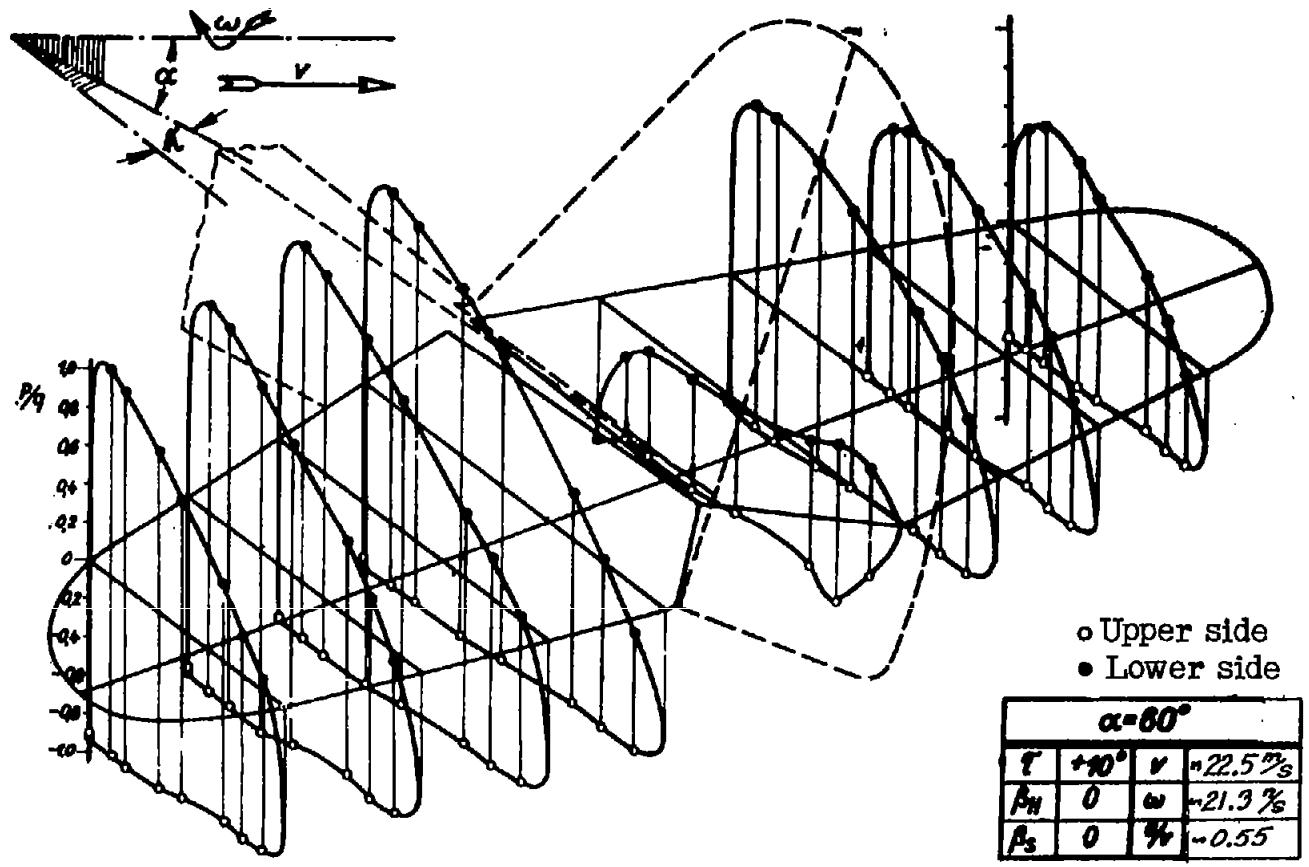
ω
α
v
h
p/q
1.0
0.8
0.6
0.4
0.2
0
-0.2
-0.4
-0.6
-0.8
-1.0
o Upper side
• Lower side
α=60°
τ
+10°
v
≈22.5 m/s
β_H
0
ω
≈21.3 m/s
β_S
0
a/v
≈0.55

Figure 29.

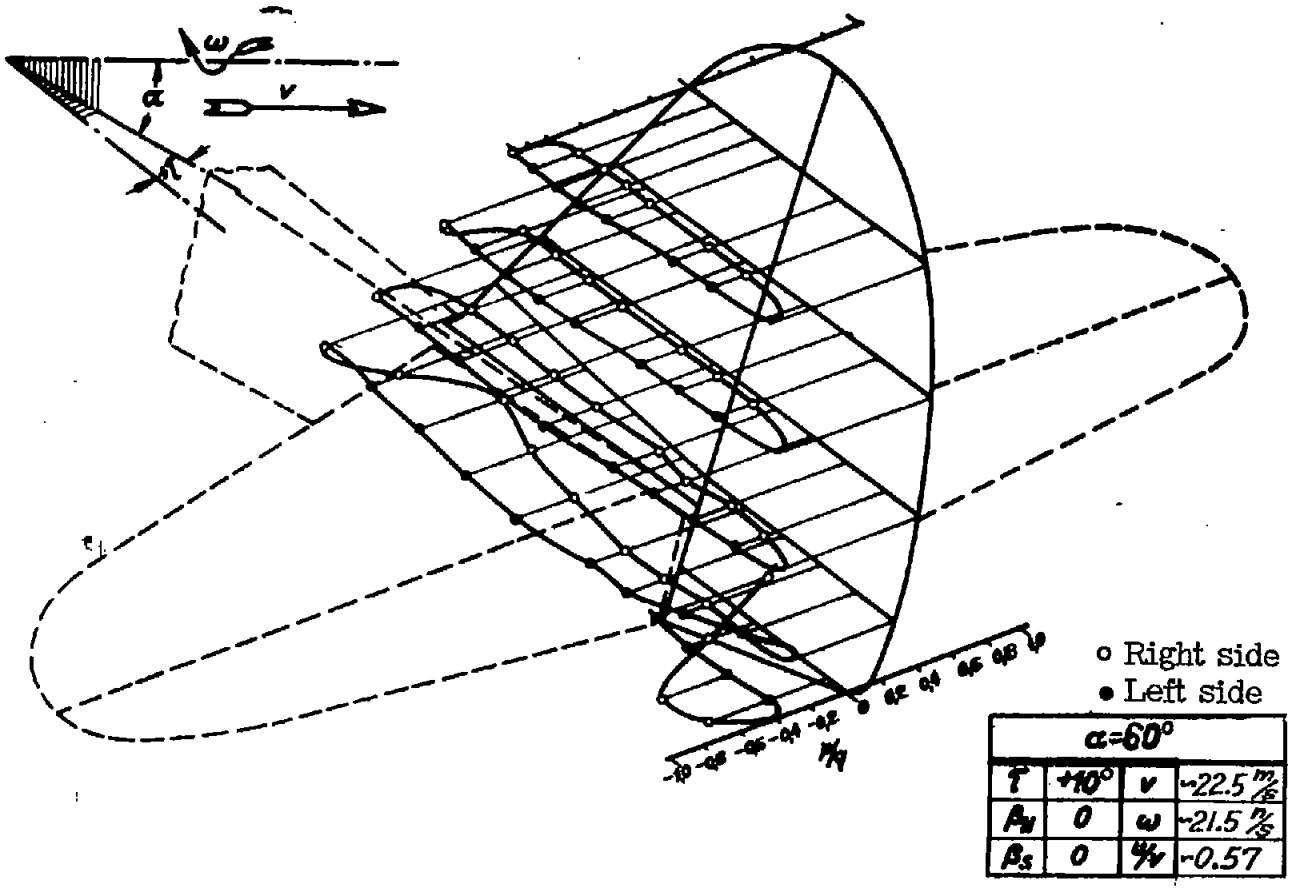
ω
α
v
τ
-1.0 -0.8 -0.6 -0.4 -0.2 0 0.2 0.4 0.6 0.8 1.0
p/q
o Right side
• Left side
α=60°
τ +10° v ~22.5 m/s
β_N 0 ω ~21.5 n/s
β_S 0 ω/v ~0.57

Figure 30.